การกลั่นแบบมีปฏิกิริยาระหว่างเอมิลแอลกอฮอล์กับกรดอะซิติก โดยใช้แอมเบอลิส15, โดเวกซ์ และ เบตาซีโอไลท์ เป็นตัวเร่งปฏิกิริยา

นางสาวอัญชัญ แพถนอม

วิทยานิพนธ์นี้เป็นส่วนหนึ่งของการศึกษาตามหลักสูตรปริญญาวิศวกรรมศาสตรมหาบัณฑิต
สาขาวิชาวิศวกรรมเคมี ภาควิชาวิศวกรรมเคมี
คณะวิศวกรรมศาสตร์ จุฬาลงกรณ์มหาวิทยาลัย
ปีการศึกษา 2552

Reactive distillation of amyl alcohol with acetic acid over Amberlyst 15, Dowex and Zeolite-Hβ

Ms. Anchan Paethanom

A Thesis Submitted in Partial Fulfillment of the Requirements
for the Degree of Master of Engineering Program in Chemical Engineering
Department of Chemical Engineering
Faculty of Engineering
Chulalongkorn University
Academic Year 2009

Thesis Title	REACTIVE DISTILLATION OF AMYL ALCOHOL WITH ACETIC ACID OVER AMBERLYST 15, DOWEX AND ZEOLITE-Hβ
By	Ms. Anchan Paethanom
Field of Study	Chemical Engineering
Thesis Advisor	Professor Suttichai Assabumrungrat, Ph.D.

Accepted by the Faculty of Engineering, Chulalongkorn University in Partial Fulfillment of the Requirements for the Master's Degree

.... Dean of the Faculty of Engineering
(Associate Professor Boonsom Lerdhirunwong, Dr.Ing.)

THESIS COMMITTEE

.... Chairman
(Associate Professor Muenduen Phisalaphong, Ph.D.)

.... Thesis Advisor
(Professor Suttichai Assabumrungrat, Ph.D.)

.... Member
(Associate Professor Supakanok Thongyai, Ph.D.)

.... Member
(Associate Professor Navadol Laosiripojana, Ph.D.)

อัญชัญ แพถนอม : การกลั่นแบบมีปฏิกิริยาระหว่างเอมิลแอลกอฮอล์กับกรดอะซิติกโดยใช้แอมเบอลิส15, โดเวกซ์ และ เบตาซีโอไลท์ เป็นตัวเร่งปฏิกิริยา. (**REACTIVE DISTILLATION OF AMYL ALCOHOL WITH ACETIC ACID OVER AMBERLYST 15, DOWEX AND ZEOLITE-Hβ**) อ. ที่ปรึกษาวิทยานิพนธ์หลัก : ศาสตราจารย์ ดร. สุทธิชัย อัสสะบำรุงรัตน์, 79หน้า.

งานวิจัยนี้ศึกษาปฏิกิริยาการสังเคราะห์นอร์มอลแอมิลอะซิเตทจากแอมิลแอลกอฮอล์และกรดอะซิติก โดยงานวิจัยได้แบ่งออกเป็นสองส่วน ในส่วนแรกเป็นการทดลองการเร่งปฏิกิริยาโดยใช้เบต้าซีโอไลต์ เป็นตัวเร่งปฏิกิริยาเพื่อหาสมการแสดงอัตราการเกิดปฏิกิริยาและทำการจำลองสมรรถนะของเครื่องปฏิกรณ์แบบกะเพื่อเปรียบเทียบสมรรถนะในการเร่งปฏิกิริยาของตัวเร่งปฏิกิริยาต่างชนิดกันซึ่งได้แก่ เบต้าซีโอไลต์ แอมเบอลิส 15 และ โดเว็กซ์ ที่อุณหภูมิต่างๆ และส่วนที่สองเป็นการศึกษาสมรรถนะและการออกแบบหอกลั่นแบบมีปฏิกิริยา โดยในงานวิจัยนี้ได้กำหนดให้ได้ผลิตภัณฑ์นอร์มอลแอมิลอะซิเตทที่มีความบริสุทธิ์ไม่ต่ำกว่า 98% โดยโมล การจำลองหอกลั่นแบบมีปฏิกิริยาในการศึกษานี้ใช้ชุดโปรแกรมทางการค้าชื่อแอสเปน นอกจากนี้ยังศึกษาถึงพลังงานที่ต้องใช้ในปฏิกิริยาและวิเคราะห์ความคุ้มค่าด้านเศรษฐศาสตร์ด้วย ผลการศึกษาพบว่าสมการแสดงอัตราการเกิดปฏิกิริยาที่เหมาะสมที่สุดคือรูปแบบแลงเมียร์-ฮินเชลวูด โดยพลังงานกระตุ้นและค่าความร้อนของการดูดซับคือ 73.71 และ 40.95 กิโลจูลต่อโมล ตามลำดับ และผลจากการศึกษาแบบจำลองพบว่า ตัวเร่งปฏิกิริยาที่เหมาะสมที่สุดสำหรับปฏิกิริยาการสังเคราะห์นอร์มอลแอมิลอะซิเตทในเครื่องปฏิกรณ์แบบกะ คือเบต้าซีโอไลต์ และระบบหอกลั่นแบบมีปฏิกิริยาที่ติดตั้งอุปกรณ์แยกวัฏภาค (decanter) เป็นระบบที่เหมาะสม และสำหรับการศึกษาในระดับอุตสาหกรรม พบว่า เมื่อพิจารณาค่าใช้จ่ายต่อปีสำหรับกรณีการใช้กรดอะซิติกเจือจาง 35% โดยน้ำหนักเป็นสารตั้งต้นและใช้แอมเบอลิส 15 เป็นตัวเร่งปฏิกิริยา พบว่าการใช้ระบบหอกลั่นแบบมีปฏิกิริยาที่ติดตั้งอุปกรณ์แยกวัฏภาค (decanter) และมีจำนวนชั้นของปฏิกิริยา 15 ชั้น จำนวนชั้นของสติปปิ้ง 6 ชั้น และเรคติฟายยิง 1 ชั้น เสียค่าใช้จ่ายต่อปีน้อยที่สุด

ภาควิชา.....วิศวกรรมเคมี..............
สาขาวิชา....วิศวกรรมเคมี.............
ปีการศึกษา........2552..................

ลายมือชื่อนิสิต.........อัญชัญ แพถนอม.........
ลายมือชื่ออาจารย์ที่ปรึกษา.............................

5070644021 : MAJOR CHEMICAL ENGINEERING
KEYWORDS : AMYL ACETATE / REACTIVE DISTILLATION / ACETIC ACID / SIMULATION / TOTAL ANNUAL COST

ANCHAN PAETHANOM : REACTIVE DISTILLATION OF AMYL ALCOHOL WITH ACETIC ACID OVER AMBERLYST 15, DOWEX AND ZEOLITE-Hβ. ADVISOR : PROF. SUTTICHAI ASSABUMRUNGRAT, Ph.D., 79 pp.

This work is to investigate the esterification reaction of amyl alcohol with acetic acid. This research is divided into two parts; experimental studies to find the kinetic rate of the amyl acetate esterification catalyzed by beta zeolite and simulation studies which is separated into two section; first, batch reactor, to compare between the results of the reaction of three catalysts; beta zeolite, Amberlyst 15 and Dowex at each temperature and second, reactive distillation which various process configurations and operating variables were investigated. All simulation results were based on the same product specification that the bottom stream contained amyl acetate with a concentration not less than 98 mol%. The commercial ASPEN PLUS program is used to simulate and their energy consumption and economic analysis are also investigated. For the kinetic studies, it was found that the Langmuir-Hinshelwood activity based model apparently shows the best kinetic model. The activation energy and the heat of adsorption of water are 73.71 and 40.95 kJ/mol respectively. From the simulation, beta zeolite showed the best performance in the batch reactor. The reactive distillation equipped with a decanter is a suitable column configuration. However, when considering the total annual cost for the case using Amberlyst 15 as a catalyst with 35 wt% acetic acid feed, it was revealed that the reactive distillation equipped with a decanter consisting of 1 rectifying, 15 reaction, and 6 stripping stages offers the lowest total annual cost.

Department ....Chemical Engineering...... Student's signature ...Anchan Paethanom
Field of Study ..Chemical Engineering..... Advisor's signature ....
Academic year ....2009...............

ACKNOWLEDGEMENTS

The author wishes to express her sincere gratitude and appreciation to her advisor, Prof. Dr. Suttichai Assabumrungrat, and also Asst. Prof. Dr. Worapon Kiatkittipong, for their valuable suggestions, stimulating, useful discussions throughout this research and devotion to revise this thesis, otherwise it cannot be completed. In addition, the author would also be grateful to Associate Professor Muenduen Phisalaphong, as the chairman, and Associate Professor Supakanok Thongyai, and Assistant Associate Professor Navadol Laosiripojana as the examiners of the thesis committee. The financial supports from Graduate school of Chulalongkorn University are gratefully acknowledged.

Most of all, the author would like to express her highest gratitude to her family especially her parents who are always supportive and pay attention to her. The most success of graduation is devoted to them.

Finally, the author wishes to thank the members of the Center of Excellence on Catalysis and Catalytic Reaction Engineering, Department of Chemical Engineering, Faculty of Engineering, Chulalongkorn University for their assistance.

CONTENTS

Page

CHAPTER

Page

Page

LIST OF TABLES

TABLE **Page**

LIST OF FIGURES

FIGURE **Page**

FIGURE **Page**

FIGURE **Page**

NOMENCLATURES

a_i	activity of species *i*	[-]
A	surface membrane area	[m^2]
D	liquid distillate flowrate	[mol/s]
Di	diffusivity coefficient	[m/s]
E_a	activation energy	[J/mol]
C	concentration of species *i*	[wt%]
c_i	concentration of species *i*	[mol/m^3]
c_{pl}	heat capacity of liquid	[J/mol.K]
F	feed flowrate	[mol/s]
F_i	molar flow rate of species *i* in the reaction side	[mol/s]
H	enthalpy	[J/s]
AcAc	acetic acid	[-]
AmAc	amyl acetate	[-]
AmOH	amyl alcohol	[-]
k_i	kinetic constant base on mol fraction	[mol/(s mol-H^+)]
L	liquid flowrate to return from stage 1 to stage 2	[mol/s]
M_i	molecular weight of species *i*	[kg/mol]
N_i	number of stages of reactive distillation or distillation	[mol]
Q	duty	[W]
Q_i	molar flow rate of species *i* in the permeate side	[mol/s]
r_i	reaction rate	[mol/(s kg-dry resin)]
RD	reactive distillation	[-]
RR	reflux ratio	[-]
R	gas constant (=8.314)	[J/(mol/K)]
T	operating temperature	[K]
TAC	total annual cost	[$/year]
x_i	liquid mole fraction of component *i*	[-]

X	conversion of reactant	[%]
Y	yield of product	[%]

Greeks letters

γ_i	activity coefficients of species i	[-]

Subscripts

Cond	condenser
i	species i
Reb	reboiler
Rec	rectifying section
Rxn	reaction section
Strp	stripping section

CHAPTER I
INTRODUCTION

1.1 Introduction

In chemical process manufactures and industries, acetic acid is a by-product in various chemical processes for instance; cellulose esters which are used in fiber processing, lacquers and photographic in film process. Cellulose acetate is synthesized by acetylation of cellulose by acetic acid, acetic anhydride and sulfuric acid as a reagent. This reaction results in the formation of a large amount by-product acetic acid containing waste, normally 35% w/w aqueous solution of acetic acid. Terephthalic acid production produces by-product containing 65% w/w of acetic acid in water. The synthesis of glyoxal from acetaldehyde and nitric acid generates by-product containing 13-20% w/w of acetic acid. The process of dimethyl telephtalate production which uses acetic acid as a surface coating chemical for resin preparation and acetic acid occurs in an aqueous stream. In the production of vinyl acetate monomer (VAM), which is cracked from ethylidene duacetate (EDA) (generated by reaction of acetic acid anhydride with acetaldehyde), acetic acid is also produced as a by-product. Large amount of acetic acid needs to be recovered.

There are numeral methods to recover acetic acid. Among these, the direct esterification reaction of acetic acid with various alcohols such as methanol, ethanol, propanol, *n*-butanol, *n*-amyl alcohol and hexanol for accessing acetate esters is a well known procedure.

Amyl acetate is one of the most important organic solvents. It is used in large quantities for various applications for example; as an extractant, a solvent and a polishing agent. Amyl acetate helps in the removal of many plastic-based stains, such as plastic glues and adhesives. It is also effective on correction fluids such as Liquid

Paper and effectively removes any residues left on garments. The consumption of amyl acetate is growing in the present.

Amyl acetate is commonly synthesized in liquid phase through esterification of acetic acid with amyl alcohol, which is catalyzed by strong acids. The reaction of amyl acetate synthesis is usually reversible and that is the difficulty in producing purity product as required. Besides, it is an equilibrium limited reaction. To improve separation and obtain enhanced conversion, simultaneous removal of products during the reaction is favorable. Various methods of product removal, such as reactive extraction and reactive distillation, have been widely studied.

Reactive distillation is the combination of distillation and reaction in a single vessel. The reaction undergoes at favorable pressure and temperature levels and needs to be catalyzed by strong acids or some solid acidic catalyst, e.g. ion exchangers. Reactive distillation offers many advantages for instance; improved selectivity, better temperature control, increased conversion, and effective utilization of reaction heat and avoidance of azeotrope. For this reaction, it is apparent that alcohol is soluble in water while ester is almost insoluble. This system is associated with the formation a minimum boiling ternary azeotrope of acetate ester, alcohol, and water in nonreactive zone, the heterogeneous azeotrope can be obtained as the distillate product. Moreover, after the vapor condensation, the aqueous phase is almost pure water and conveniently withdrawn as product while the organic phase can be recycled back as reflux.

For equilibrium limited reactions, there are ranges of operating condition which are suitable for both the reaction and separation enable the use of reactive distillation. Reactive distillation has become an attractive unit operation in recent years because of its potential for capital productivity improvements, selectivity improvements due to a fast removal of reactants or products from the reaction zone, due to exothermic reaction that the reaction heat can be used for vaporization of liquid or elimination of solvents in the process, reduce the number of equipment unit as two process steps can be carried out in the same vessel compared to conventional reactor-separation sequences, and lower capital and operating cost.

The ternary azeotropic mixture between amyl acetate, amyl alcohol and water is formed as a low-boiling ternary azeotrope, considering the thermodynamic properties of the reaction system. If the distillated overhead can be cooled down to sufficiently low temperature, a suitable condition to break azeotrope, the ternary azeotrope can be eliminated. Amyl acetate is a high boiling point product and also a heavy key component in the production of acetate ester by esterification via reactive distillation. Amyl acetate is withdrawn from the bottom of the column. Two phase separation is allowed when the overhead distillate, consisting of amyl alcohol, water, and Amyl acetate is condensed and cooled to a temperature sufficiently low. Decanter based separation process can be applied in the separation of liquid azeotropes. Its applications can be found in dehydration of organic/water mixtures, removal or recovery of organic compounds from water, and separation of organic mixture. In general, decanter has been used for separation of organics from water, resulting in consideration of the combination of reactive distillation with other unit operations.

In this work, experiment and simulation are carried out to investigate the result of reactive distillation of esterification reaction of acetic acid with amyl alcohol. The reactions were performed over three different types of catalyst which are Amberlyst 15, Dowex and Zeolite-Hβ. They have been tested and their results compared. Various reactive distillation based systems are also considered because the presence of high water content in the acetic acid feed. To help the water removal in the system, a decanter unit is included in the process. The commercial Aspen Plus program is used to simulate the performances of the different systems to find suitable process configuration and operating conditions.

CHAPTER II

THEORY

2.1 Amyl Acetate Synthesis

Amyl acetate is commonly synthesized by the esterification of acetic acid and amyl alcohol as shown in Equation 2.1. It is a reversible kinetically controlled reaction which is catalyzed by free protons. Sulfuric acid or sulfonic acid ion-exchange resins are commonly used as catalyst.

$$\underset{\text{(acetic acid)}}{CH_3COOH} + \underset{\text{(amyl alcohol)}}{C_5H_{11}OH} \leftrightarrow \underset{\text{(amyl acetate)}}{CH_3COOC_5H_{11}} + \underset{\text{(water)}}{H_2O} \qquad (2.1)$$

Table 2.1 Properties of each chemical

	AmOH	**AcAc**	**AmAc**	**H_2O**
Name	Amyl alcohol, 1-Pentanol, n-pentanol, pentan-1-ol	Acetic acid, ethanoic acid,	Amyl acetate, pentyl ethanoate, pentyl acetate	water
Molecular formula	$C_5H_{12}O$	$C_2H_4O_2$	$C_7H_{14}O_2$	H_2O
Molar mass	88.15 g/mol	60.05 g/mol	130.19 g/mol	18.02 g/mol
Density	0.8144 g/cm^3	1.049 g/cm^3	0.876 g/cm^3	1000 kg/m^3
Melting point	-77.6 °C	16.5 °C	-71 °C	0 °C
Boiling point	137.986 °C	118.1 °C	149 °C	100 °C
Solubility in water	22 g/l	Fully miscible	10 g/l	Fully miscible
Viscosity		1.22 mPa·s		1 mPa·s

According to thermodynamic properties of amyl acetate esterification system, amyl acetate as the high boiling point product is obtained as the bottom product in a reactive distillation process. The 1-pentanol-water-amyl acetate, 1-pentanol-water, and amyl acetate-water azeotropes have similar boiling points, and therefore, 1-pentanol, amyl acetate, and water are the main components present in the distillate.

Dilute acetic acid is produced in large quantities in many processes such as manufacture of cellulose esters, terephthalic acid, and dimethyl terephthalate. The recovery of acetic acid from these streams is a problem. The conventional methods of recovery are azeotropic distillation, simple distillation, and liquid-liquid extraction. With the advantages of reactive distillation processes, esterification of acetic acid with methanol seems to be an attractive alternative. Apart from esterification with methanol, esterification with other alcohols may also be used for recovery. Many authors have explored the possibility of esterifying acetic acid from aqueous solution with n-butanol in a reactive distillation column. In this case one gets an overhead product consisting of a ternary heterogeneous azeotrope of 1-pentanol, amyl acetate, and water.

2.2 Catalysts

Zeolite-Hβ is white, odorless and powder catalyst. The advantages of this catalyst possesses, such as acidic properties, shape-selectivities, environment friendly nature of catalysts, the easy work-up, the high purity of the products, and the recycling of catalysts. Zeolite-Hβ has been used as an acid catalyst in organic chemical conversion such as alkylation20 and acylation. This catalyst is reported to have Brønsted acid sites in the micropores and on the external surface, and Lewis acid sites predominantly at the internal surface due to the local defects. Dowex is an acidic cation-exchange resin. Amberlyst 15 is strongly acidic, macroreticular, with fully sulphonated cation exchange resin catalyst.

2.3 Reactive Distillation

Integrating reaction and separation processes, reactive distillation is currently being used as a unit operation to enhance conversion of reactions that are equilibrium-limited. The two largest-scale and most well-known products of reactive distillation technology are MTBE (methyl-*tert*-butyl ether, a gasoline component replacing lead compounds) and methyl acetate (used for the production of photographic films).

When designed correctly, reactive distillation columns can overcome equilibrium limitations by removing the product out of the reaction zone and in turn forcing the reaction to complete conversion. Moderately exothermic reactions are considered ideal to be carried out in reactive distillation columns because the heat of reaction can be used to heat the column and thus drive separation. In this case the device makes ideal use of the energy produced in the reaction lowering environmental costs.

At the same time reactive distillation can bypass distillation boundaries such as azeotropes by reaction. Distillation boundaries appear because vapor and liquid have the same composition. This makes any composition change by distillation impossible. The equality of concentration in vapor and liquid phase does not limit concentration changes due to reaction.

As first reactive distillation systems have reached maturity leading to large-scale commercial production. The focus of basic engineering research into these systems has shifted. Due to the high amount of integration, column parameters are more strongly linked reducing the degrees of freedom for design. Special problems arise with scale-up and a general scale-up method is still not available. The degree of complexity of designing reactive distillation columns increases further if phase splitting into two liquid phases can occur within the system or if one of the reactants is a non-condensable gas like hydrogen for hydrogenation reactions or oxygen for oxidation reactions. Strong interaction of operating parameters can also lead to much interesting and nonintuitive column behavior making such columns harder to operate.

Finally first ideas are being forwarded to couple several reactive distillation columns to achieve reactive separation effects.

Reactive distillation allows a chemical reaction and multistage distillation to take place simultaneously in a column. The combined unit operation, especially suits for chemical reactions where reaction equilibrium limits the conversion in a conventional reactor to a low-to-moderate level. By continuously separating products from reactants while the reaction is carried out, the reaction can proceed to much higher level of conversion. Since this demonstration of its ability to render cost-effectiveness and compactness to some chemical plants, reactive distillation has been explored as a potentially important process for several reactions. Along with esterification and etherification, other reactions such as acetalization, hydrogenation, alkylation, and hydration have been explored. The objectives of existing and potential applications of reactive distillation are to: surpass equilibrium limitation, achieve high selectivity towards a desired product, achieve energy integration, perform difficult separations, and so on. Apart from its application as a multifunctional reactor, reactive distillation can be looked upon as an efficient separator for the recovery or purification of chemicals. The reversible reactions such as esterification and acetalization can be exploited for this purpose. The component to be removed is allowed to react in the distillation column and the resultant product can be separated simultaneously. One or more of these benefits are offered by the processes with reactive distillation.

2.3.1 Reactive Distillation Configurations

A conventional configuration for a chemical process usually involves two steps of chemical reaction and subsequent separation. In the chemical reaction step, reactants are brought into contact with solid catalysts at appropriate process conditions in one or more reactors. The stream leaving the reactor section then goes to one or more separation steps where unconverted reactants are separated from the products of the reaction and the inerts. The unconverted reactants, in some cases, may be recycled to the reaction section. When a substantial amount of inerts are present in the system, at least two separation units for separation of high purity product and for separation of the unconverted reactants from the inerts are required. The separation process in distillation is typically chosen.

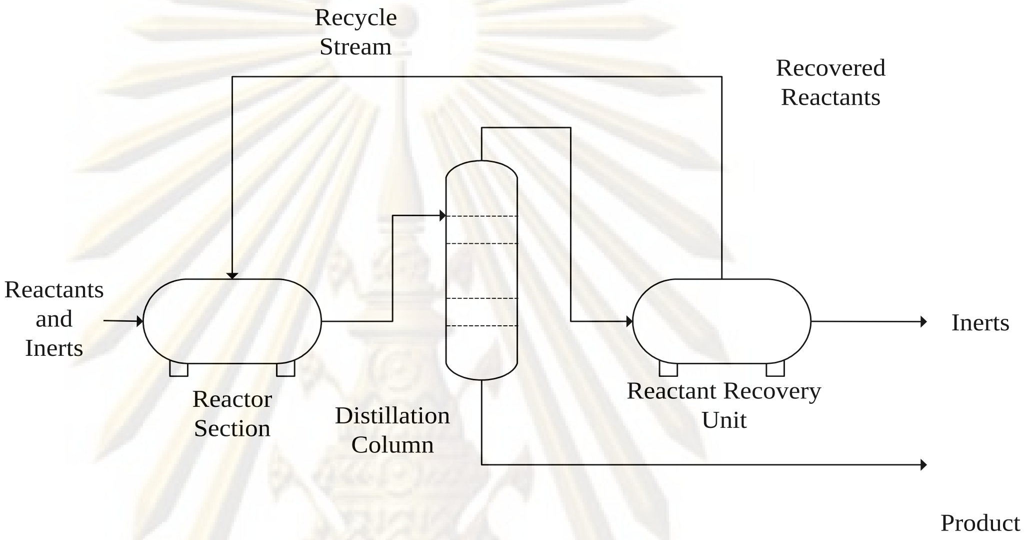

Figure 2.1 Conventional process involving reaction followed by separation

A conventional process configuration is shown in Figure 2.1 where a distillation is used for separation. In the case, a reaction product is less volatile than reactants and inert. The flow diagram of the application of reactive distillation to this process is shown in Figure 2.2. The middle section of the column is the reactive distillation section. For a non-azeotopic chemical system, separation of the inerts takes place in the rectification section of the column and the purification of the product takes place in the stripping section.

In the other configuration, the reaction and distillation proceed in alternating steps. The reactive distillation column contains both the catalyst contact device and the distillation device. A reaction occurs in the catalyst contact device and then the reacting phase passes to the distillation device for vapor/liquid contact and separation. These two steps occur alternately. By making the steps of infinitely small size, this configuration becomes equivalent to the first one. For both configurations, a rectification section may be located above the reactive distillation section of the column and a stripping section may be located below it, depending upon purity specifications.

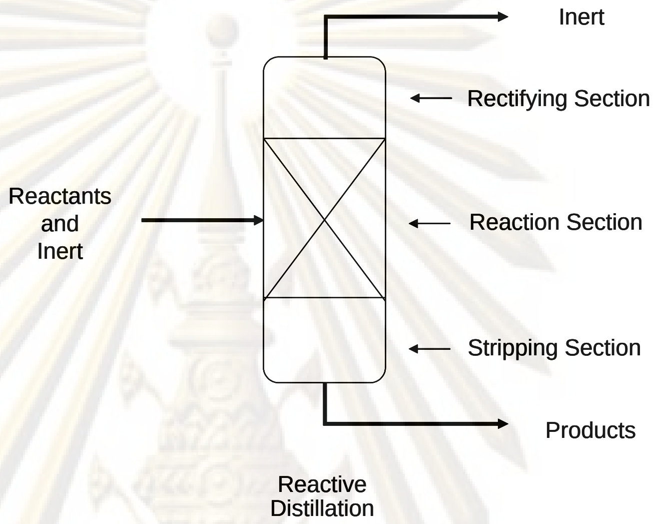

Figure 2.2 Application of reactive distillation for low volatility product process.

2.3.2 Advantages of Reactive Distillation

Application of reactive distillation to a catalytic chemical reaction using solid catalysts offers many advantages compared to a conventional process, for example:

- Two process steps i.e. separation and reaction, can be carried out in the same device. Such integration leads to lower costs in pumps, piping and instrument.
- The heat released from the reaction can be used for vaporization of liquid, leading to savings of energy costs by the reduction of reboiler duties.
- The maximum temperature in the reaction zone is limited to the boiling point of the reaction mixture, so that the danger of hot spot

formation on the catalyst is reduced significantly. A simple and reliable temperature control can be achieved.

- Product selectivity can be improved due to a fast removal of reactants or products from the reaction zone. By this, the probability of consecutive reactions, which may occur in the sequential operation mode, is lowered.
- If the reaction zone in the reactive distillation column is placed above the feed point, poisoning of the catalyst can be avoided. This leads to longer catalyst lifetime compared to conventional systems.

2.4 Aspen Plus Program

Aspen Plus program is one of the components in the Aspen Engineering Suite. It is an integrated set of products designed specifically to promote best engineering practices and to optimize and automate the entire innovation and engineering workflow process throughout the plant and across the enterprise. It automatically integrates process models with engineering knowledge databases, investment analyses, production optimization and numerous other business processes. Aspen Plus contains data, properties, unit operation models, built-in defaults, reports and other features. Its capabilities develop for specific industrial applications, such as petroleum simulation.

Aspen Plus is easy to use, powerful, flexible, process engineering tool for the design and steady-state simulation and optimization of process plants. Process simulation with Aspen Plus can predict the behavior of a process using basic engineering relationships such as mass and energy balances, phase and chemical equilibrium, and reaction kinetic. Given reliable thermodynamic data, realistic operating conditions and the rigorous Aspen Plus equipment models, actual plant behavior can be simulated. Aspen Plus can help to design better plants and to increase profitability in existing plants.

2.4.1 Features of Aspen Plus Program

Utilize the latest software and engineering technology to maximize engineering productivity through its Microsoft Windows graphical interface and its interactive client-server simulation architecture.

- Contain the engineering power needed to accurately model the wide scope of real-world applications, ranging from petroleum refining to non-ideal chemical systems containing electrolytes and solids.
- Support scalable workflow based upon complexity of the model, from a simple, single user, process unit flowsheet to a large, multi-engineer developed, multi-engineer maintained, plant-wide flowsheet.
- Contain multiple solution techniques, including sequential modular, equation-oriented or a mixture of both, and allow as quick as possible solution times regardless of the application.

2.4.2 Benefits of Aspen Plus Program

- Proven track record of providing substantial economic benefits throughout the manufacturing life cycle of a process, from R&D through engineering and into production.
- Allow users to leverage and combine the power of sequential modular and Equation-oriented techniques in a single product, potentially reducing computation times by an order of magnitude while at the same increasing the functionality and suability of the process model.
- Compete effectively in an exacting environment to remain competitive in Process currently industries it is necessary to do more, often with smaller staffs and more complex process

2.5 Estimating Costs

Operating costs are normally simple to estimate. Once we know the flow rate of the raw material streams and the utility flows (fuel, steam, cooling water, power, etc.), we simply multiply the flow by the dollar value of that stream. Care must be taken that the utility values are given on a thermodynamically consistent basis; i.e. fuel and electricity should be more expensive than high pressure steam, which should be more expensive than low pressure steam, etc. After we have determined the stream flows and stream temperature, we can calculate the equipment sizes. Of course, the total processing costs are interested so we must be able to predict the installed equipment costs, rather than the purchased equipment costs.

The total annual cost (TAC) is summation of operating cost and capital cost per year. The total annual cost determined by Douglas, 1988 is used to evaluate the appropriateness of a design. The total annual cost is defined as

$$\mathrm{TAC} = \text{operating cost} + \frac{\text{capital cost}}{\text{pay - back period}} \tag{2.2}$$

CHAPTER III
LITERATURE REVIEWS

Reactive distillation is an interesting alternative to some conventional processes, especially for equilibrium-limited reactions such as esterification and etherification. In this reaction, products are continuously removed from the reaction mixture. Thus, conversion and selectivity are increasing. Esterification reactions are important synthesis processes in chemical industries and it is possible that the reactive distillation process will progressively replace the conventional ester production processes. The esterification reaction of acetic acid and alcohol is one of the processes applying reactive distillation technology. Amyl acetate is one of the most important acetate ester which is organic solvent. It is used in large quantities for various applications for example; as an extractant, a solvent and a polishing agent and other branches of chemical industry. Several researchers have studied the reactive distillation behavior amyl acetate esterification.

3.1 Recovery of Dilute Acetic Acid

Acetic acid aqueous solutions are produced as by-products of many important processes, such as in the manufacture of cellulose esters, terephthalic acid and dimethyl terephthalate. Furthermore, reactions involving acetic anhydride either as a reagent (e.g. acetylations) or as a solvent (e.g. nitrations) can produce a large amount of acetic acid containing waste. Among the industrially relevant examples, the process for the manufacture of cellulose acetate from acetylation of cellulose by acetic acid, acetic anhydride and sulphuric acid, is typically associated with a 35% w/w aqueous solution of acetic acid as a waste stream. Terephthalic acid process involves the concentrations even up to 65% w/w of acetic acid in water (Van Brunt, 1992). The process for the synthesis of glyoxal from acetaldehyde and nitric acid has a relatively dilute acetic acid stream (typically 13–20% w/w) as a by-product. The wood distillate contains much lower concentrations (1–8% w/w) of acetic acid (Wagner et al., 1991).

A different route is to convert dilute acetic acid into useful chemicals such as acetates, which has been explored by several researchers (Xu et al., 1999; Saha et al., 2000; Hung et al., 2005). Generally, reactive distillation is used for converting dilute acid into acetate and the conversion of the acid ranges from 60-80% as shown in the studies of Saha et al., 2000 and Xu et al., 1999. Hung et al., 2005 explore the process chemistries based on the total annual cost (TAC) and they conclude that amyl alcohol is an ideal solvent for converting the dilute acid to amyl acetate and this offers great economic potential as compared to the cost of acetic acid.

3.2 Kinetics of Amyl Acetate Synthesis Reaction

A number of models have been proposed for correlating the kinetic data. The pseudo-homogeneous model (Tsao et al., 1968; Xu et al., 1995; Rihko et al., 1997; Gonzalez and fair, 1997) is the simplest one to describe the kinetic behavior of a heterogeneous reaction. This model is similar to the power law model for homogeneous reactions (Venimadhavan et al., 1994). Starting from the Langmuir-Hinshelwood rate function, Xu and Chuang, 1996 derived a quasi-homogeneous model to correlate the kinetic data by assuming that the surface reaction was the rate-controlling step and the adsorption was weak for all components. The resultant model is in the same form as the pseudo-homogeneous model. The Langmuir-Hinshelwood model and the Eley Rideal model are commonly used, when the rate-limiting step is the surface reaction between adsorbed molecules. Rihko and Krause, 1995 and Linnekoski et al., 1997 have found that the Langmuir-Hinshelwood model yielded the best results for representing etherification of TAEE and the Eley-Rideal model for that of TAME. Although complicated models may give better results, the number of adjustable parameters in the models usually becomes greater. The adjusted parameters from data fitting, if excessive, can lose their physical significance.

The kinetic behavior of heterogeneous esterification of acetic acid with amyl alcohol was investigated at temperatures from 303.15 K to 353.15 K over an acidic cation exchange resin catalyst, Amberlyst 15 (Lee M. J et al., 1999). The kinetic data were correlated by a quasi-homogeneous model with which the apparent rate constants at each reaction temperature were determined. The activation energies of the forward and the backward reactions were found to be 51.74 kJ/mol and 45.28 kJ/mol, respectively. As evidenced from experimental results, the equilibrium conversion of acetic acid and the apparent equilibrium constant increase with increasing temperature, implying that the esterification is endothermic.

Lee et al., 2000 has been studied more about kinetic behavior of amyl alcohol over an acidic cation-exchange resin, Dowex 50Wx8-100 has been studied. The experiments were conducted in a fixed-bed reactor at temperatures from 323 to 393 K and at molar ratios of feed (amyl alcohol to acetic acid) from 1 to 10. The equilibrium conversion of acetic acid was found to increase with increasing reaction temperature. The kinetic data were correlated with the quasi-homogeneous, Langmuir-Hinshelwood, Eley-Rideal, and modified Langmuir-Hinshelwood models. It is found that the modified Langmuir-Hinshelwood model yielded the best representation for the kinetic behavior of the reaction over wide ranges of temperature and feed composition.

3.3 Application of Reactive Distillation for Amyl Acetate Synthesis

The concept of combining reaction and separation has long been recognized (Doherty and Buzad, 1992), but rarely put into commercial practice, not until the successful application for the production methyl acetate. Despite clear advantages of simultaneous reaction/separation (Kaymak and Luyben, 2004), commercializing of reactive distillation processes is still quite limited for several reasons. An obvious one is mentioned in Doherty and Buzad, 1992, “There is almost always a conventional alternative to reactive distillation which is seductive because we have always done it this way”. The scenario remains more than a decade later. After the management and technical levels were convinced by the clear edge of reactive distillation, another reason is that the process flowsheets seem to change from case to case.

The recovery of acetic acid from its dilute aqueous solutions is a major problem in both petrochemical and fine chemical industries. The conventional methods of recovery are azeotropic distillation, simple distillation and liquid–liquid extraction. Physical separations such as distillation and extraction suffer from several drawbacks. The esterification of an aqueous solution (30%) of acetic acid with amyl alcohol is a reversible reaction. As excess of water is present in the reaction mixture, the conversion is greatly restricted by the equilibrium limitations. The amyl acetate ester has a wide range of applications. In view of the appreciable value of amyl acetate ester, there were many works which were directed towards recovery of 30% acetic acid by reaction with amyl alcohol in a reactive distillation column using ion-exchange resin as a catalyst. Experiments were conducted in order to achieve an optimum column configuration for the synthesis of amyl acetate in a reactive distillation. The effect of various parameters, e.g. total feed flowrate, length of catalytic section, reflux ratio, mole ratio of the reactants, location of feed points and effect of recycle of water were studied.

Amyl acetate has been used in industries as a solvent, an extractant, a polishing agent etc. Design and control of amyl acetate using pure acetic acid has been studied by Chiang et al., 2002 and Huang and Yu, 2003 and mentioned that amyl acetate reactive distillation columns have been designed for “neat” operation. That is an exact stoichiometric amount of alcohol and acid is processed in one column such that high purity product can be obtained with an almost 100% conversion, as opposed to excess reactant design. This imposes stringent requirements on the control system design.

The acetic acid esterifications with five different alcohols, ranking from methanol to amyl alcohol (C1 to C5), using the reactive distillation, were investigated (Tang et al., 2005). The optimization results showed an interesting fact that different flowsheets gave rise to different dominant optimization variables and the TAC’s of different flowsheets were compared. Hung et al., 2006 studied the feasibility of recovery of acetic acid from aqueous solutions with different acid concentrations.

Instead of separating acid from water using azeotropic distillation, acetic acid is converted to acetate via esterification. A range of acetic acid concentrations is explored, varying from 100 wt%, to 75 wt%, to 50 wt%, and then to 30 wt%. The TAC analysis shows that a standalone reactive distillation is more economical than a flow sheet with a pre-treatment unit. Process characteristics have been explored and the results show significant nonlinearity associated with reactive distillation columns for all four different acid concentrations. Acceptable control performance can be obtained while maintaining acetate composition.

CHAPTER IV

EXPERIMENTAL AND SIMULATION

This chapter describes the experimental and simulation procedure for the synthesis of amyl acetate from amyl alcohol and acetic acid in semi batch reactor and via reactive distillation system. This work is divided into two parts; experimental studies to find the kinetic rate of the amyl acetate esterification catalyzed by Beta Zeolite and simulation studies which is separated into two section; first, batch reactor, to compare between the results of the reaction in of three catalysts; Beta Zeolite, Amberlyst 15 and Dowex at each temperature and second, reactive distillation in which various process configurations and operating variables of the reactive distillation systems were investigated in order to find their effects on reaction performances as well as their energy consumption and economic analysis. The computer simulations were carried out using Aspen Plus program. Details are given in the following sections.

4.1 Kinetic Study

The reaction of amyl acetate synthesis from acetic acid and amyl alcohol can be shown below.

$$\text{AmOH} + \text{AcAc} \underset{k_b}{\overset{k_f}{\rightleftharpoons}} \text{AmAc} + \text{H}_2\text{O} \qquad (4.1)$$

4.1.1 Batch Reactor Apparatus

The autoclave type reactor is cylindrical shape with outside and inside diameter of 5 and 4 cm, respectively and 8 cm of height. It can stand operating pressure as high as 30 atm. The turbine for mixing and valve for liquid sampling including the thermocouple are installed at the top. The mixture was stirred at the maximum speed of 1163 rpm in all the runs to minimize the external mass transfer resistance. Figure 4.1 shows the semi batch reactor apparatus. The experiments carried out at high pressure to ensure all reaction components were always in liquid phase.

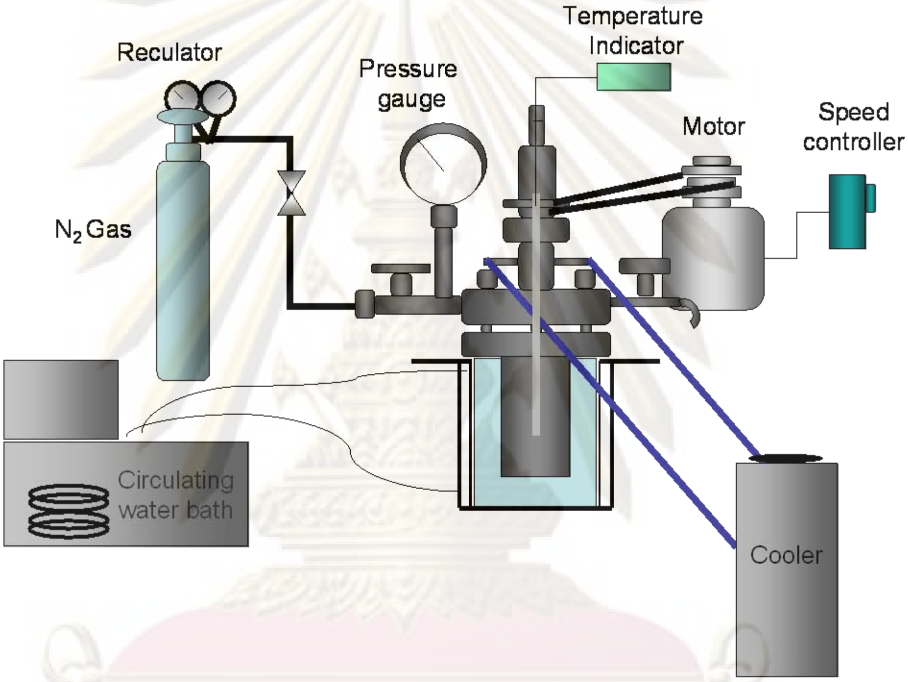

Figure 4.1 Schematic diagram of the catalyst selection experimental set-up

4.1.2 Chemical and Catalyst

The chemicals used in this study consist of standard grade chemicals with purify higher than 99.5% for gas chromatograph calibration and reagent grade chemicals for major experiments. Table 4.1 provides details of the levels of purity and suppliers. The commercial catalyst Beta Zeolite was used in the study. The catalyst was dried overnight in an oven at 383 K before use. Table 4.2 provides the properties of Beta Zeolite catalyst.

Table 4.1 Details of chemicals use in the study

Chemical materials	Purity (%)	Supplier
Amyl acetate	99.8	Merck KGaA Chemical
Amyl alcohol	99.5	Merck KGaA Chemical
Acetic acid	100.0	Merck KGaA Chemical

Table 4.2 Catalyst properties

Beta Zeolite	980HOA
Cation Type	H
SiO_2/Al_2O_3(mol/mol)	540
Na_2O(wt%)	0.1
Surface Area(BET, m_2/g)	400
Crystal Size(μm)	0.05
Mean Particle Size(μm)	2

4.1.3 Experimental Procedure

1. 50 cm^3 of acetic acid, 50 cm^3 of amyl alcohol and 5 g of catalyst were added into the reactor together at room temperature.
2. The solution was pressurized by N_2 gas to 4 atm to prevent vaporization of liquid solutions and heated to the desired reaction temperature (333, 343 and 353 K) and stirred at about 1163 rpm.
3. Liquid samples (0.5 cm^3) were taken for analysis every hour. It was noted that, approximately about 1 cm^3 of sample was drained before sampling because it had some residue in the sampling part.

4.1.4 Analysis

The analysis was carried out using gas chromatography (GC). The operating condition of the GC is shown in Table 4.3.

$1x10^{-3}$ cm^3 of sample was injected into the GC and the raw data of chromatogram was modified by using calibration curve (see details in Appendix B) and conversion, selectivity and yield of amyl acetate synthesis were calculated. It should be noted that a sample must be centrifuged before use in order to separate residue catalyst which can damage the GC column.

Table 4.3 Operating conditions of gas chromatography

Gas Chromatography Shimadzu GC			
Operating Conditions			
Detector	TCD	Mesh size of Packing	60/80
Carrier Gas	He (99.98 %)	Injection temperature (K)	443
Carrier Gas Flow rate (cm3/min)	30	Column temperature (K)	473
Packed Column	Gaskuropack 54	Detector temperature (K)	473
Length of Column (m)	2.5	Current (A)	80
Integration Parameter			
Width (sec)	5	Slope (uV/min)	30
Drift (uV.min)	0	T. DBL (min)	1000
Stop Time (min)	75	Atten (2^X mV)	5
Speed (mm/min)	2		
Quantitative Parameters			
Method (0-8)	1	Curve (Calib. Fit Type)	0
Cal. Levl (0-15)	1	Min.Area (count)	100
Win. Band (0:win 1: Band)	0	Window (%)	5
Spl. Wt	100	IS. Wt	0
Dilfact	1		

4.2 Catalyst Performance Comparison

The reaction rate expressions of amyl acetate esterification catalyzed by Amberlyst 15 and Dowex which could be found in the literatures (Lee et al., 1999 and Lee et al., 2000, respectively) and by Beta Zeolite catalyst obtained from the experiment above, their catalyst performance at various temperature, 360, 380 and 400 K can be compared by simulation in a batch reactor by mole change with time.

4.3 Reactive Distillation Study

The simulation studies in this work were divided into two scales of reactive distillation systems, i.e., pilot and industrial scales. The reactive distillation column was simulated by using Aspen Plus program. The steady state RADFRAC model was used for the amyl acetate production in the reactive distillation columns. The base case of this work was set at the following condition: no pressure drop in the column (1 atm), pressure of feed stream of 1 atm, temperature of feed stream of 298 K, the feed position of amyl alcohol and acetic acid at the first and the fourth stage of reaction, respectively, total condenser and Kettle reboiler. The order of column stages was assigned from the top to the bottom of the column, with stage 1 as the condenser and stage N as the reboiler. All simulation results were based on the same product specification that the bottom stream contained amyl acetate with a concentration not less than 98 mol%.

The reversible esterification of amyl alcohol and acetic acid occurred at the reaction section in the reactive distillation. Kinetic rate constants of both the forward and backward reactions were necessary information for simulations. For Aspen Plus program, the kinetic rate constants based on concentration or mole fraction are required. This work used the kinetic rate constants of the reaction on Amberlyst 15 and Dowex catalyst in concentration form from the literatures (Lee et al., 1999 and Lee et al., 2000, respectively) and on Beta Zeolite catalyst from the experiment in section 4.1, its kinetic rate constants for both forward and backward reaction in concentration form were calculated.

Table 4.4 Kinetic rate constants based on concentration of Amberlyst 15 and Dowex catalysts.

Catalyst	Kinetic rate constants	
Amberlyst 15	$k_\mathrm{f} = \exp\left(10.347 - \frac{6223}{T}\right)$	(4-2)
	$k_\mathrm{b} = \exp\left(7.720 - \frac{5446}{T}\right)$	(4-3)
Dowex	$k_\mathrm{f} = \exp\left(5.926 - \frac{5266}{T}\right)$	(4-4)
	$k_\mathrm{b} = \exp\left(3.297 - \frac{4490}{T}\right)$	(4-5)

4.3.1 Pilot Scale: Effect of Decanter

According to the previous work (Hung et al., 2006), the reactive distillation in a pilot scale unit for amyl acetate esterification from concentrate acetic acid and amyl alcohol contains totally 41 stages (including reboiler) which consists of 1 rectifying, 33 reactive and 6 stripping stages. This column configuration was used for preliminary simulation study in order to investigate effects of operating variables on performance of the reactive distillation system. Feed flow rate of pure amyl alcohol and acetic acid was kept at 50 kmol/h for single reactive distillation. The reactive distillation columns of amyl acetate synthesis catalyzed by Amberlyst 15 with and without a decanter (shown in Figure 4.2) were considered at different values of reboiler heat duty (Q) and reflux ratio (L/D) to study the significant of decanter. Then, the suitable reactive distillation system was used to find optimal design variables for the operation of the reactive distillation.

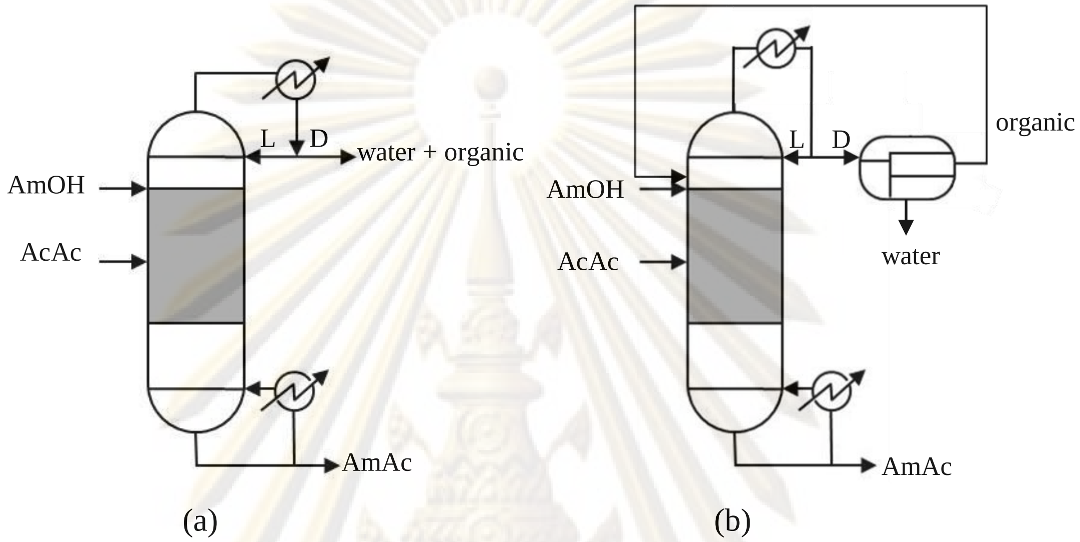

Figure 4.2 Single reactive distillation system for comparison between (a) only reactive distillation, (b) the reactive distillation equipped with decanter.

4.3.2 Industrial Scale: Economic Study of the Optimal Configuration of Each Catalyst

The simulations of amyl acetate in an industrial scale were aimed to determine an optimal configuration of the system by taking into account capital and operating costs. Feed flow rate of the pure amyl alcohol and acetic acid was kept at 50 kmol/h. The single-column reactive distillation was investigated to determine effects of design variables such as the number of rectifying, reaction and stripping stages (using the suitable system configuration from the results of the pilot scale study). Acetic acid concentration of 35 wt% were used to react with amyl alcohol with each type of catalyst (Amberlyst-15, Dowex and Beta Zeolite) in a single reactive distillation column for design of the column and finding of the minimal cost. All details of simulations, sizing of equipment and quantity of material in this part were described in Appendix D and total annual cost of the system was calculated from Equation 2.2.

4.4 Conversion of Reactant and Yield of Product

All system performances were considered in terms of conversion of acetic acid (X_{AcAc}), and yield of amyl acetate (Y_{AmAc}) defined as follows;

$$X_{\mathrm{AcAc}} = \frac{\text{Differencein molar flow rate of inlet and outlet of AcAc} \times 100}{\text{Molar feed flow rate of AcAc}} \tag{4.6}$$

$$Y_{\mathrm{AmAc}} = \frac{\text{Molar flow rate of outlet of AmAc} \times 100}{\text{Molar feed flow rate of AcAc}} \tag{4.7}$$

CHAPTER V

RESULTS AND DISCUSSION

5.1 Kinetic Study

5.1.1 Reaction Equilibrium Constants

The reaction of the esterification between acetic acid and amyl alcohol to get amyl acetate is shown in Equation 5.1.

$$\text{AmOH} + \text{AcAc} \underset{k_b}{\overset{kf}{\rightleftharpoons}} \text{AmAc} + \text{H}_2\text{O} \qquad (5.1)$$

From the equation, the reaction equilibrium constant can be defined as;

$$K_{eq} = \frac{k_f}{k_b} \qquad (5.2)$$

where f = forward reaction and b = backward reaction

The reaction equilibrium constant in term of concentration reported in the literature (Lee et al., 1999) is shown in Equation 5.3.

$$K_{eq,c} = 13.83 \exp\frac{-776.1}{T} \qquad (5.3)$$

Gibbs energy of formation was used to determine the equilibrium parameter in activity form. The solution is shown in Appendix C.

$$K_{eq,a} = exp\left(-1.471 + \frac{1118.568}{T}\right) \qquad (5.4)$$

5.1.2 Development of Mathematical Models

The results from the kinetic study of the reaction of amyl acetate synthesis from acetic acid and amyl alcohol were fitted to two kinetic models; Langmuir-Hinshelwood (L-H) and Power Law model (PL) based on activities (a_i) and concentration (c_i), abbreviated as LH-A, PL-A for activity and PL-C for concentration. The LH model is based on the following assumptions; all components adsorb on the single site of the catalyst and the surface reaction is the rate determining step. As a result, the rate law of the reaction can be expressed in term of activity and concentration as

- Power Law model based on concentration and activity

$$-r_c = k_{f,c}\left(c_{AmOH}\, c_{AcAc} - \left(1/K_{eq,c}\right) c_{AmAc}\, c_{H_2O}\right) \qquad (5.5)$$

$$-r_a = k_{f,a}\left(a_{AmOH}\, a_{AcAc} - \left(1/K_{eq,a}\right) a_{AmAc}\, a_{H_2O}\right) \qquad (5.6)$$

- Langmuir-Hinshelwood model based on concentration and activity

$$-r_c = \frac{k_{f,c}\left(c_{AmOH}\ c_{AcAc} - \left(1/K_{eq,c}\right) c_{AmAc}\ c_{H_2O}\right)}{(1+ K_{w,c} c_{H_2O})} \qquad (5.7)$$

$$-r_a = \frac{k_{f,a}\left(a_{AmOH}\ a_{AcAc} - \left(1/K_{eq,a}\right) a_{AmAc}\ a_{H_2O}\right)}{(1+ K_{w,a} a_{H_2O})} \qquad (5.8)$$

where $k_{f,c}$ *and* $k_{f,a}$ are the forward reaction rate constants of reaction based on concentration and activity, respectively. $K_{w,c}$ and $K_{w,a}$ are the H_2O inhibition parameters based on concentration and activity, respectively.

The activity can be calculated from the following relation.

$$a_i = \gamma_i x_i \qquad (5.9)$$

where x_i is mole fraction of species *i* in the liquid mixture and γ_i is the activity coefficient which could be estimated by using UNIFAC method (see detail in Appendix A).

By performing the material balance for a batch reactor, the following equation is obtained.

$$\frac{-dN_{AmOH}}{dt} = \frac{-dN_{AcAC}}{dt} = \frac{dN_{AmAc}}{dt} = \frac{dN_{H_2O}}{dt} = w(r) \qquad (5.9)$$

where *w* and *r* represent weight of catalyst and reaction rate, respectively.

The minimizing root mean square deviation (RMSD) method was used to estimate the kinetic parameters (k_f and K_w). A MATLAB program was employed to find the best-fitted kinetic parameters which minimize the relative root mean square deviation (RMSD) values expressed by Equation 5.10.

$$RMSD_i = \frac{1}{M}\sqrt{\sum_{k=1}^{M}\left[\frac{(x_{i,k} - x_{i,exp,k}}{x_{i,exp,k}}\right]^2} \qquad (5.10)$$

where *i* and *M* represent the component and the number of experiment data point, respectively.

5.1.3 Kinetic Parameter Determination

A set of experiments was carried out at three temperature levels to investigate the kinetic parameters. The mathematical models from the previous study were used to determine the kinetic parameters. First of all, the power law based on both activity and concentration were compared to find the best rate expression for the esterification of amyl alcohol with acetic acid. Figures 5.1-5.3 show typical results of mole changes with time at T = 333, 343 and 353 K, respectively. The solid lines in the figures represent the simulation results from the PL-A model and the dash lines represent the PL-C model. It was found that the simulation results for both PL-A and PL-C kinetic model agreed quite well with the experimental results.

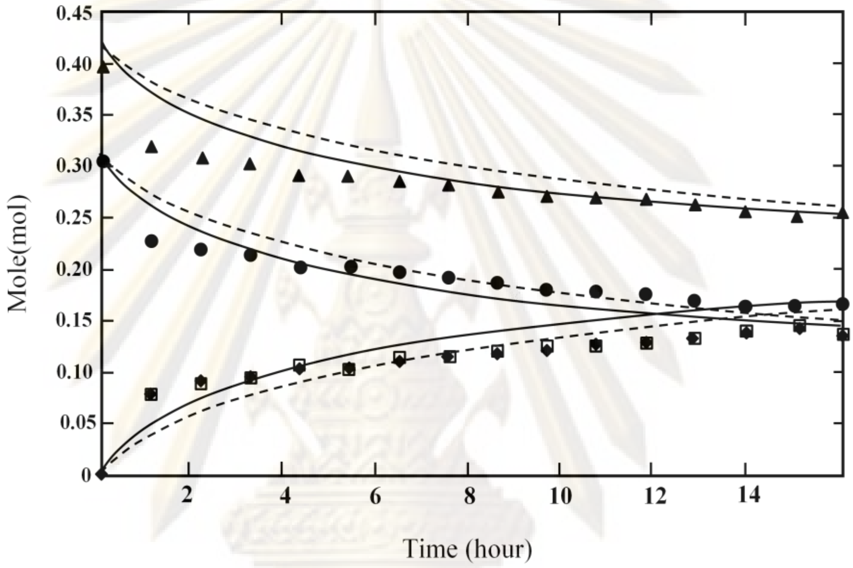

Figure 5.1 Mole change with time at 333 K (symbol: experiment result, dash line: PL-C model and solid line: PL-A model).

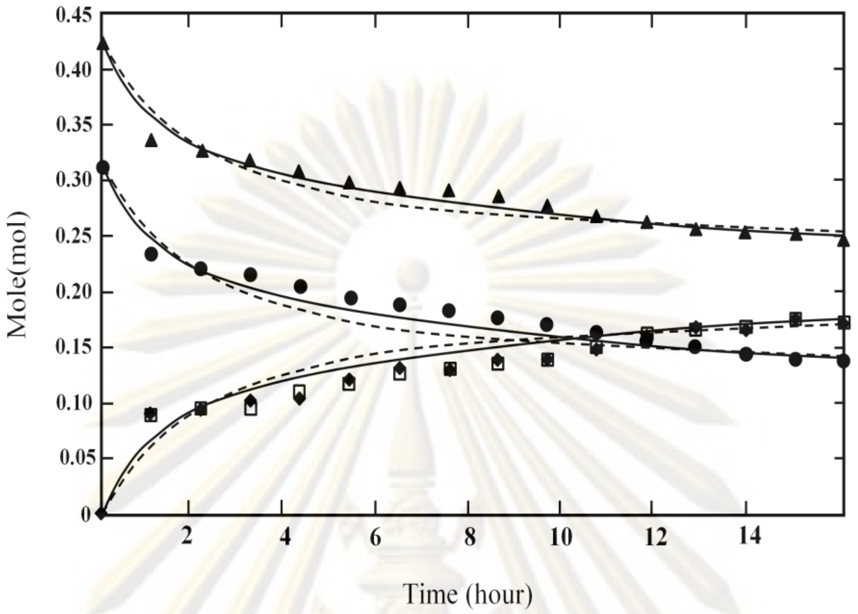

Figure 5.2 Mole change with time at 343 K (symbol: experiment result, dash line: PL-C model and solid line: PL-A model).

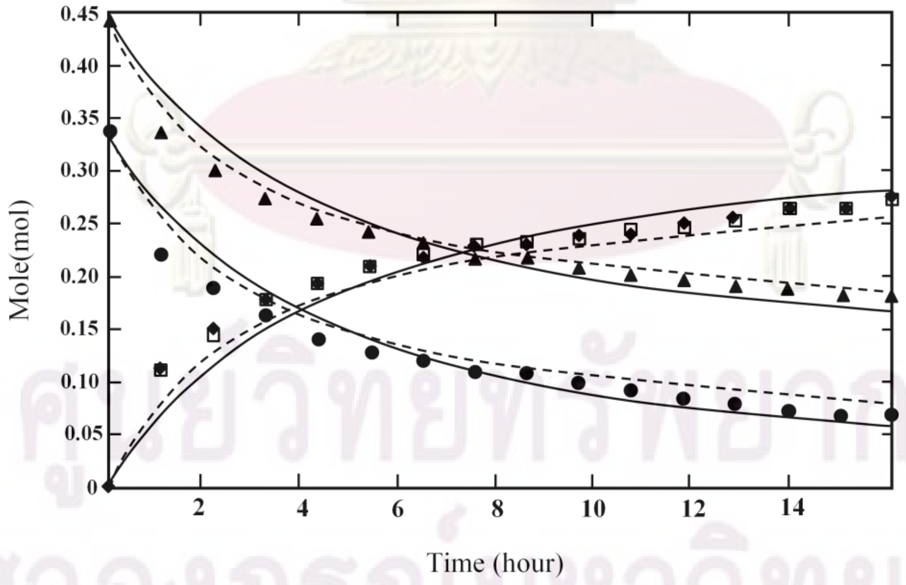

Figure 5.3 Mole change with time at 353 K (symbol: experiment result, dash line: PL-C model and solid line: PL-A model).

Moreover, the LH model was considered to find the best kinetic model for this reaction. From the previous study, both of PL-A and PL-C showed a fine performance to describe the amyl acetate esterification reaction. Figures 5.4-5.6 illustrate the experimental results of mole profile compared with the simulation result from LH-A and LH-C kinetic model of each component in the amyl acetate esterification reaction at 333, 343 and 353 K, respectively. It was found that the experimental results agreed well with the simulation results of LH-A and LH-C kinetic model. In Figure 5.7, the average RMSD values with different models were summarized, the Langmuir-Hinshelwood activity based (LH-A) model apparently shows the best kinetic model to fit the experimental results of amyl acetate esterification.

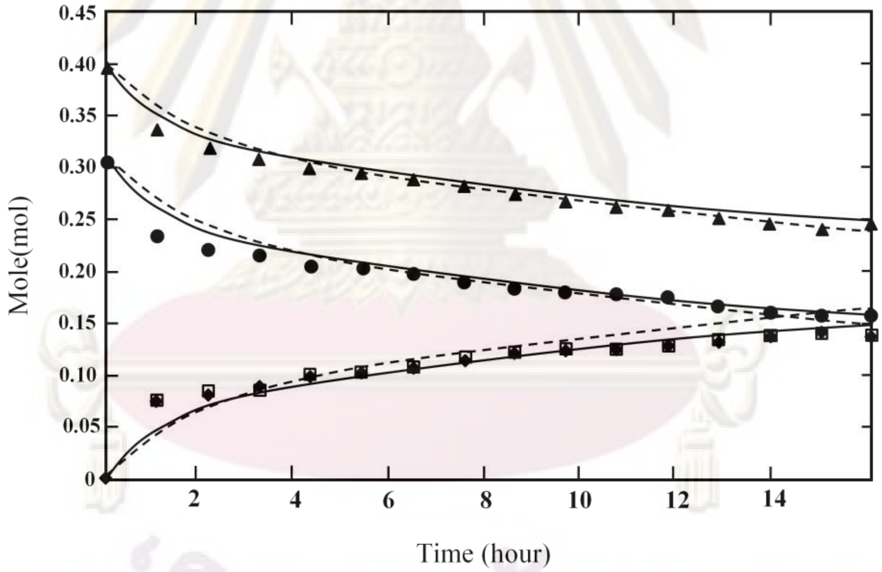

Figure 5.4 Mole change with time at 333 K (symbol: experiment result, dash line: LH-C model and solid line: LH-A model).

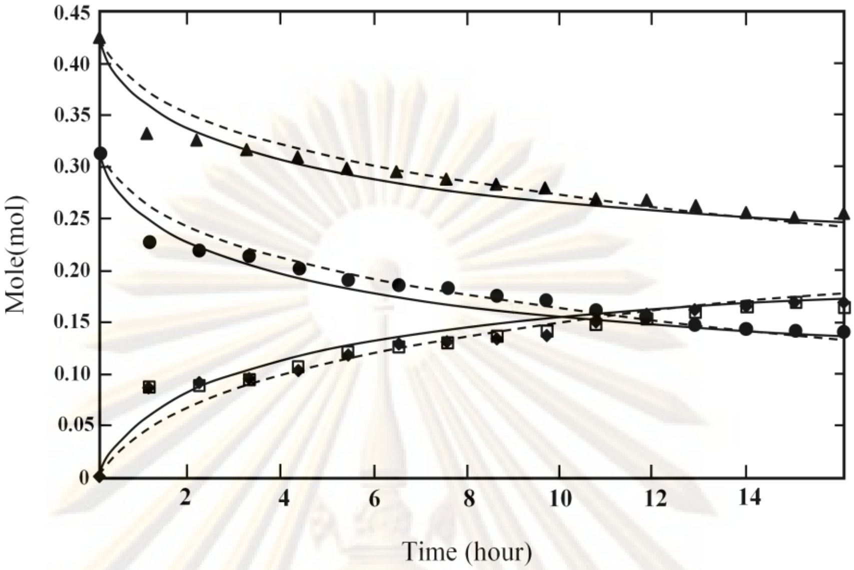

Figure 5.5 Mole change with time at 343 K (symbol: experiment result, dash line: LH-C model and solid line: LH-A model).

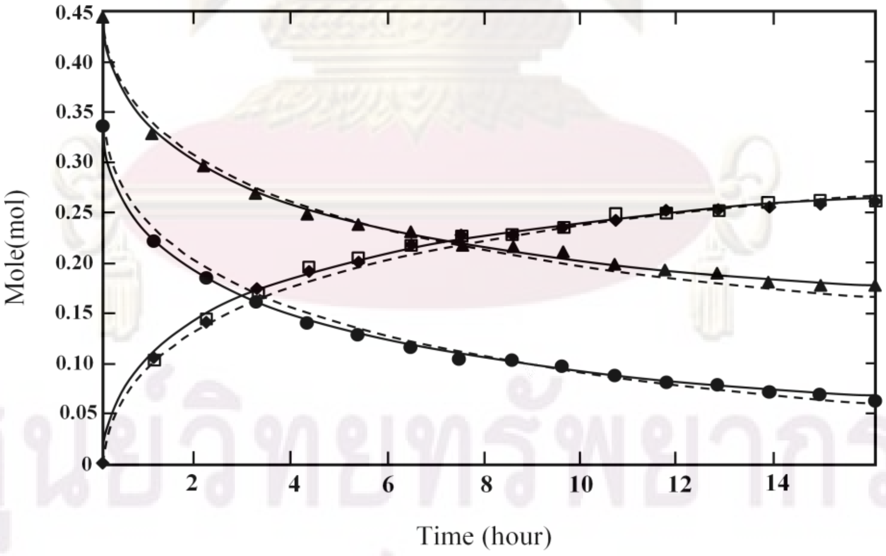

Figure 5.6 Mole change with time at 353 K (symbol: experiment result, dash line: LH-C model and solid line: LH-A model).

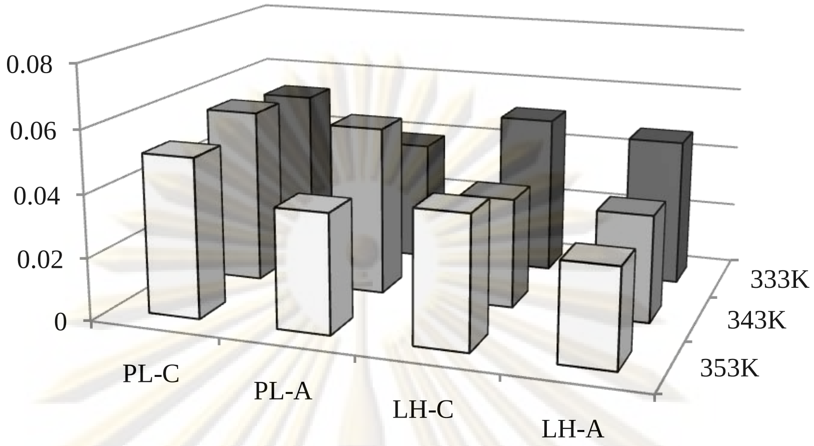

Figure 5.7 Average RMSD values of PL and LH kinetic models for both activity and concentration different temperatures

The temperature dependent rate constants were determined by plotting the relationships according to the Arrhenius equation for both Power Law and Langmuir-Hinshelwood kinetic model in activity and concentration form while the sorption equilibrium constant of water as a function of temperature can be determined by Van’t Hoff plot. Figures 5.8 and 5.9 show the plot of kinetic models based on activity and concentration, respectively. It was found that the value of sorption equilibrium of water decreased with the increasing of temperature. This is a conventional behavior observed in most of the adsorption processes. The temperature dependent rate constant and the chemical equilibrium constant of both models can be expressed by the Arrhenius equation, Equation 5.11. The sorption equilibrium constant and values of the adsorption enthalpies and adsorption entropies of water for LH-A and LH-C kinetic model can be expressed by the Van’t Hoff equation, Equation 5.12. The expressions of the rate constants, activation energies and sorption equilibrium constants are summarized in Table 5.1.

$$k_i = A_o exp\left[\frac{-E_a}{RT}\right] \tag{5.11}$$

$$K_w = exp\left[\frac{-\Delta G}{RT}\right] = exp\left[\frac{\Delta S}{R} - \frac{\Delta H}{RT}\right] \qquad (5.12)$$

where E_a is activation energy (kJ/mol), ΔH is standard enthalpy change of the reaction, ΔS is standard entropy change of the reaction, T is temperature in Kelvin and R is the gas constant.

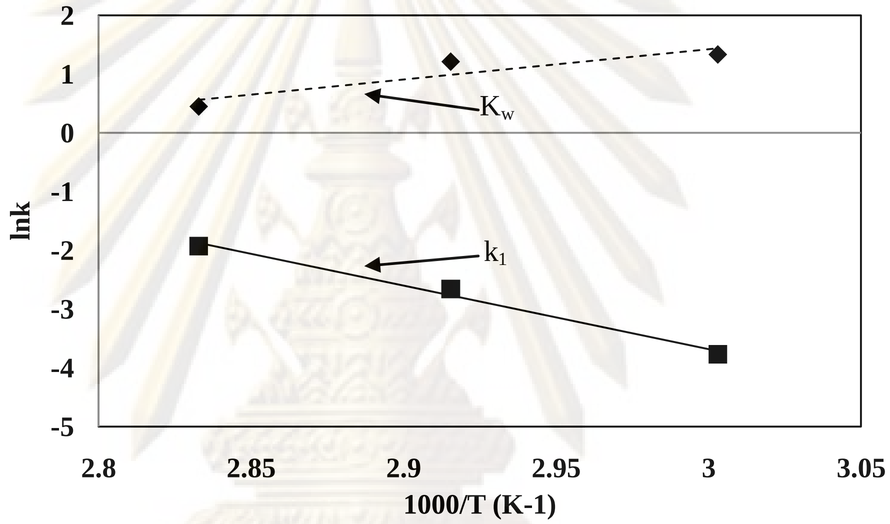

Figure 5.8 Arrhenius's (solid line) and Van't Hoff plot (dash line) of concentration based kinetic model.

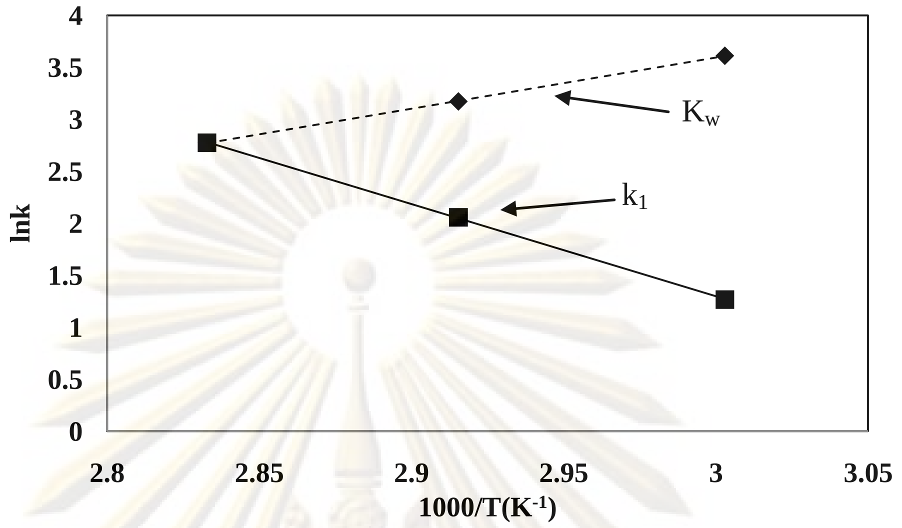

Figure 5.9 Arrhenius's (solid line) and Van't Hoff plot (dashed line) of activity based kinetic model.

Table 5.1 Kinetic parameters of PL and LH model

Model		**k (mol kg^{-1} s^{-1})**	**Ea (kJ mol^{-1})**
PL	**k_c**	Exp(3.873- (5387.64/T))	44.79
	k_a	Exp(8.071- (6317.98/T))	52.53
LH	**k_c**	Exp(28.836-(10841/T))	90.14
	k_a	Exp(27.893-(8864.9/T))	73.71
		K_w	**ΔH(kJ mol^{-1})**
	K_{wc}	Exp(-14.043+(5155.5/T))	- 42.87
	K_{wa}	Exp(-11.182+(4925.3/T))	- 40.95

5.2 Catalyst Performance Comparison

As of the reaction rate expressions of amyl acetate esterification catalyzed by Amberlyst 15 and Dowex which could be found in the literatures (Lee et al., 1999 and Lee et al., 2000, respectively) and by Beta Zeolite catalyst obtained from the experiment above, their catalyst performance at various temperature, 360, 380 and 400 K can be compared by acetic acid conversion change with time. Figures 5.10-5.12 demonstrate plotting between the conversion of acetic acid and time at each temperature.

It appears that the catalysts have the same tendency that the equilibrium conversion increases with increasing temperature due to the endothermic reaction. The equilibrium conversions of all three catalysts are almost the same while Beta Zeolite catalyst can make the conversion of acetic acid reach the equilibrium before Dowex and Amberlyst 15 catalyst, respectively.

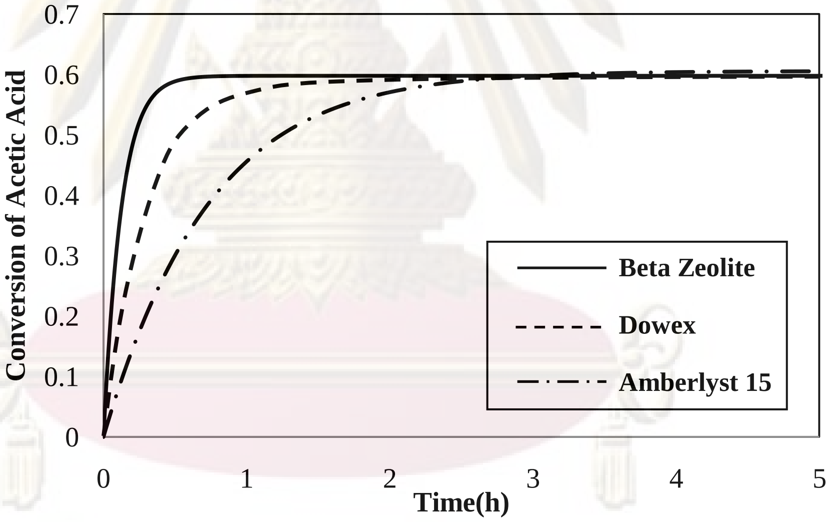

Figure 5.10 Conversion of acetic acid of Amberlyst 15, Dowex and Beta Zeolite catalysts at 360 K

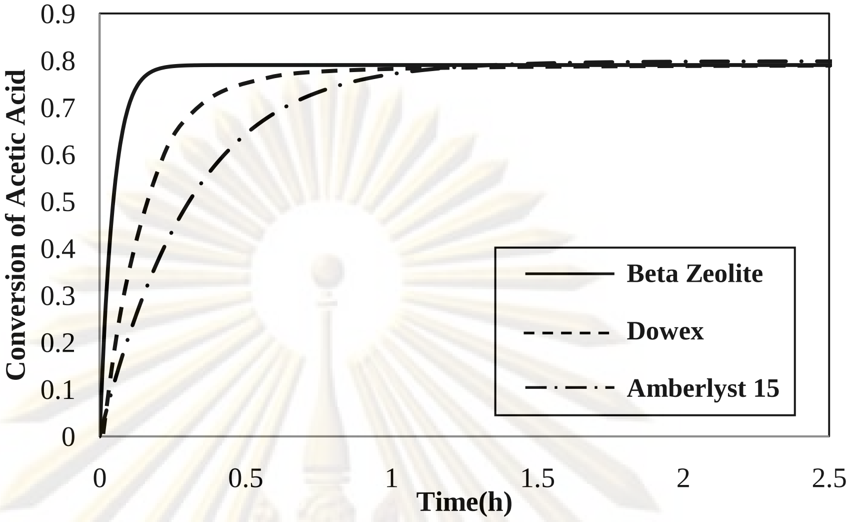

Figure 5.11 Conversion of acetic acid of Amberlyst 15, Dowex and Beta Zeolite catalysts at 380 K

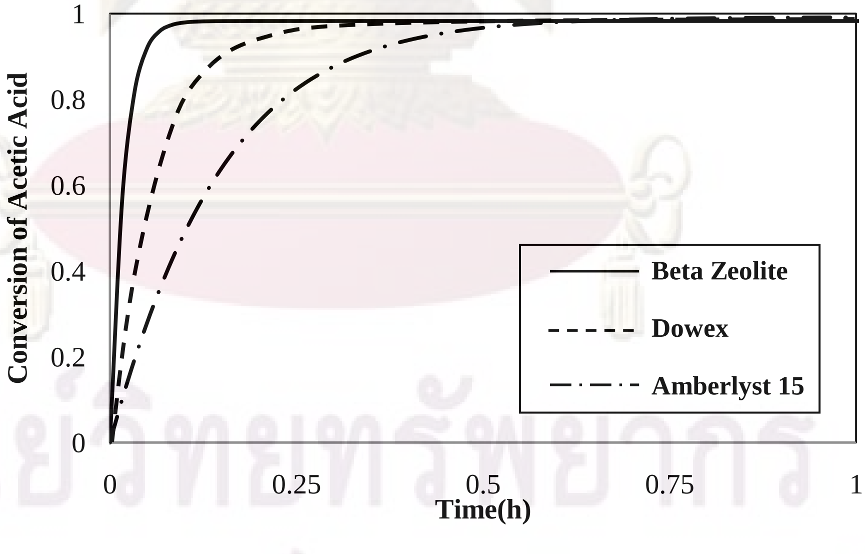

Figure 5.12 Conversion of acetic acid of Amberlyst 15, Dowex and Beta Zeolite catalysts at 400 K

5.3 Reactive Distillation Study

The simulations using Aspen plus program were carried out to investigate the amyl acetate synthesis from acetic acid and amyl alcohol in the reactive distillation. Various operating parameters; i.e. reflux ratio, heat duty, catalyst type, catalyst weight, number of the column stage and reaction zone were investigated. The rate expressions obtained from the literatures (Lee et al., 1999 and Lee et al., 2000) and previous study were significant for the program. The performance of reactive distillation at standard operating condition was described and the influence of each operating parameter was discussed.

The simulation of the esterification of acetic acid and amyl alcohol in a reactive distillation is carried out using the Aspen Engineering suit. The RADFRAC model, which is a rigorous equilibrium-stage distillation model to describe a multistage vapor-liquid separation in the distillation column in Aspen Plus simulation package is used to simulate. The property option was set as UNIFAC. The column contained a total of 41 stage counted from top to bottom included reboiler. The reactive distillation column was divided into three sections: 1 stages of rectifying section, 33 stages of reaction section and 6 stages of stripping section. The chemical reactions were assumed to occur in the liquid phase in the 33 reactive stages of the reaction zone (stage 2-34). The preliminary configuration of reactive distillation column used in the simulation studies is shown in Table 5.2 (Tang et al., 2005) with the details of the column parameters and feed conditions.

Table 5.2 Preliminary configuration for the simulation (Hung et al., 2006)

Configurations			
Total No. of trays including the reboiler	41	Acetic acid feed tray	5
No. of trays in stripping section(N_S)	6	Amyl alcohol feed tray	2
No. of trays in reactive section (N_{RXN})	33	Feed flow rate of acetic acid (kmol/h)	50
No. of trays in rectifying section (N_R)	1	Feed flow rate of amyl acetate (kmol/h)	50
Reactive trays	2-34		

5.3.1 Pilot Scale: The Effect of Decanter

In this part, the synthesis of amyl acetate from esterification of pure acetic acid (100 wt%) and amyl alcohol by a reactive distillation is investigated. A single reactive distillation system with/without a decanter, as shown in Figure 5.13, was first examined to find whether the decanter should be included in the reactive distillation process. This study used Amberlyst 15 as a catalyst to see the significance of a decanter. It is noted that the decanter is employed to separate the solution mixture from a column condenser into the aqueous phase and the organic phase. The performance of reactive distillations in terms of the conversion of acetic acid, yield and mole fraction of amyl acetate at the bottom was analyzed by varying several operating parameters, i.e., reboiler heat duty and reflux ratio. It is noted that the reflux ratio is defined as the ratio of molar flow rate of reflux stream (*L*) and distillate stream (*D*).

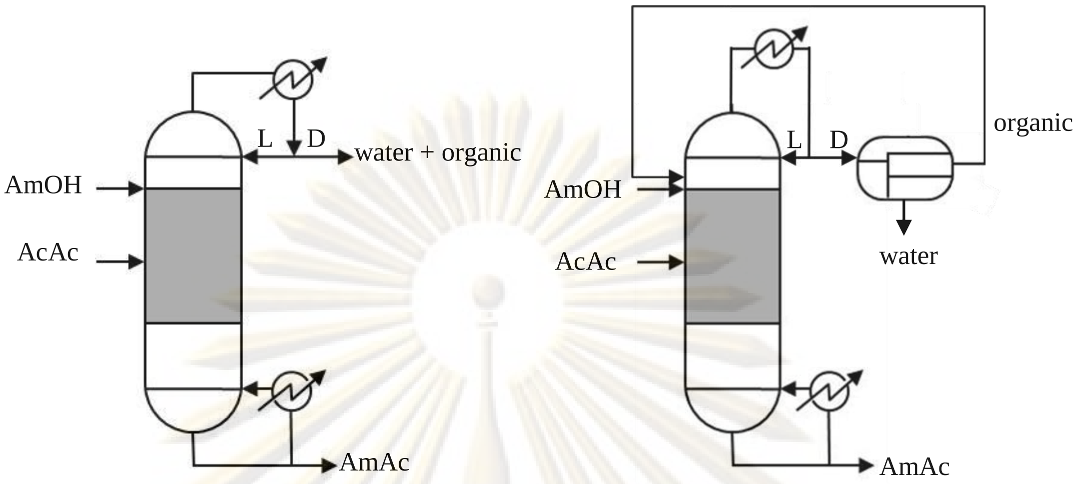

(a) (b)

Figure 5.13 Single reactive distillation system for comparison between (a) only reactive distillation, (b) the reactive distillation equipped with decanter.

5.3.1.1 Single Reactive Distillation without Decanter

Figure 5.14 presents the influence of the heat duty on the conversion of acetic acid for different values of the reflux ratio. It can be seen that increasing the reboiler heat duty results in increasing of the conversion of acetic acid for all values of reflux ratio. As heat duty increased, more acetic acid traveled up to the reactive section and then reacted with amyl alcohol, more reactants were in the reaction zone and the esterification reaction increased. Therefore, more yield and purity of the product, amyl acetate, at the bottom were observed as shown in Figures 5.15 and 5.16. The acetic acid conversion decreased with increasing reflux ratio because the increasing of reflux ratio increases the concentration of water in reaction section then the equilibrium cannot shift forward. It is noticed that although the conversion of acetic acid was high at any specific value of the reflux ratio and heat duty, the yield of amyl acetate at the bottom was still low. This is because some of the amyl acetate product was lost in the distillate stream and also from the simulation, the distillate was separated into two liquid phases, water and organic. This result suggests that the use of a decanter to separate the organic phase which contained mostly amyl acetate from the aqueous phase which water is a major component could improve the performance of the reactive distillation.

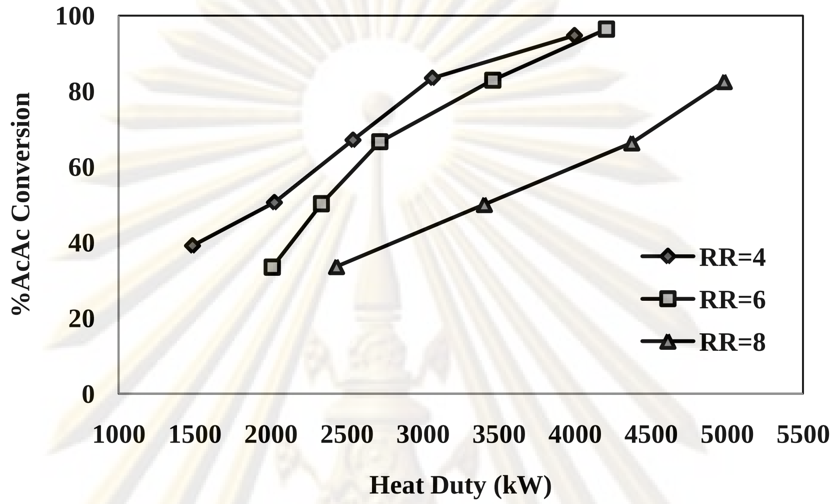

Figure 5.14 Effect of reboiler heat duty on the conversion of acetic acid at various reflux ratio values (single RD without decanter).

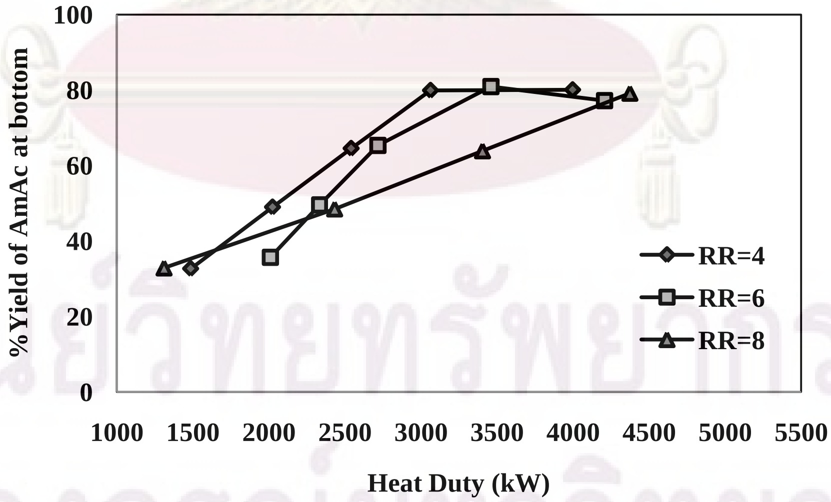

Figure 5.15 Effect of reboiler heat duty on the yield of amyl acetate at various reflux ratio values (single RD without decanter).

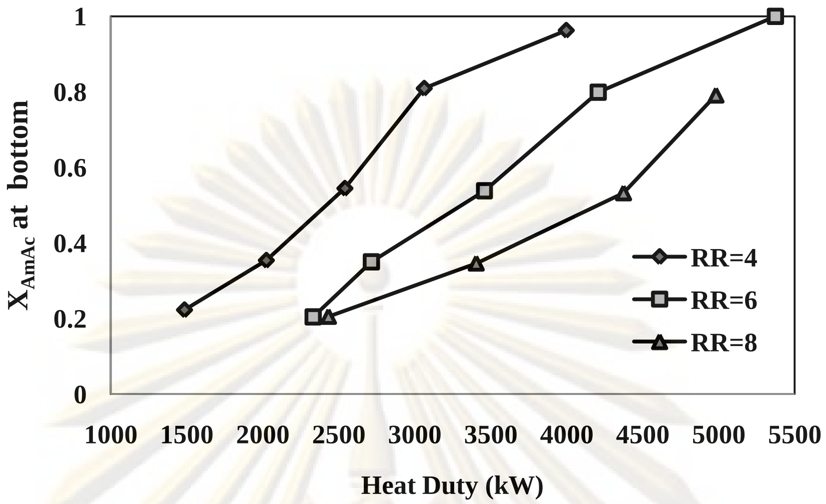

Figure 5.16 Effect of reboiler heat duty on the mole fraction of amyl acetate at bottom of the column at various reflux ratio values (single RD without decanter).

5.3.1.2 Single Reactive Distillation with Decanter

Since the distillate stream of the reactive distillation consists of organic and aqueous phase, the removal of the aqueous phase from the distillate stream could enhance the reactive distillation performance to obtain more product. Figures 5.17 to 5.19 show the effect of the reboiler duty at various reflux ratio values on the conversion of acetic acid, the yield and mole fraction of amyl acetate in the bottom, respectively. It can be seen that when the heat duty increases, it leads to increase the conversion of acetic acid, and yield and mole fraction of amyl acetate in the bottom while the increasing of reflux ratio did not seem to be important. The configuration with high reflux ratio consumed a lot of heat to achieve high acetic acid conversion while the same conversion amount could be achieved from the way less heat duty with lower reflux ratio.

From simulation results, the reactive distillation with decanter consumed less energy, compared to that of the reactive distillation column without decanter since some solution mixture in aqueous phase is separated in the decanter and drawn from the reactive distillation column as distillate.

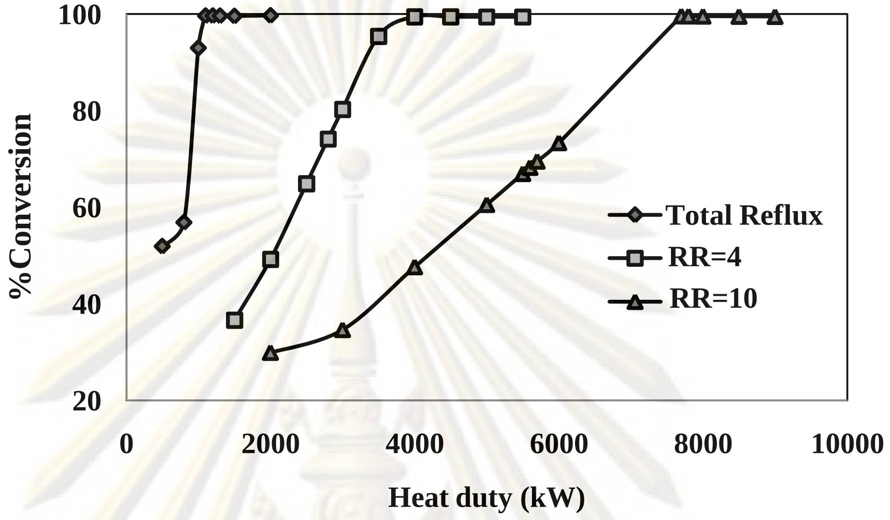

Figure 5.17 Effect of reboiler heat duty on the conversion of acetic acid at various reflux ratio values (single RD with decanter).

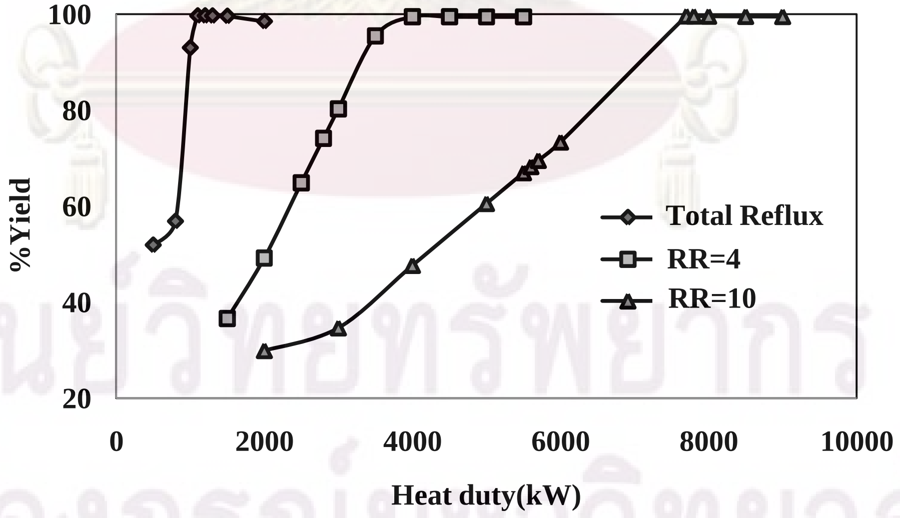

Figure 5.18 Effect of reboiler heat duty on the yield of amyl acetate at various reflux ratio values (single RD with decanter).

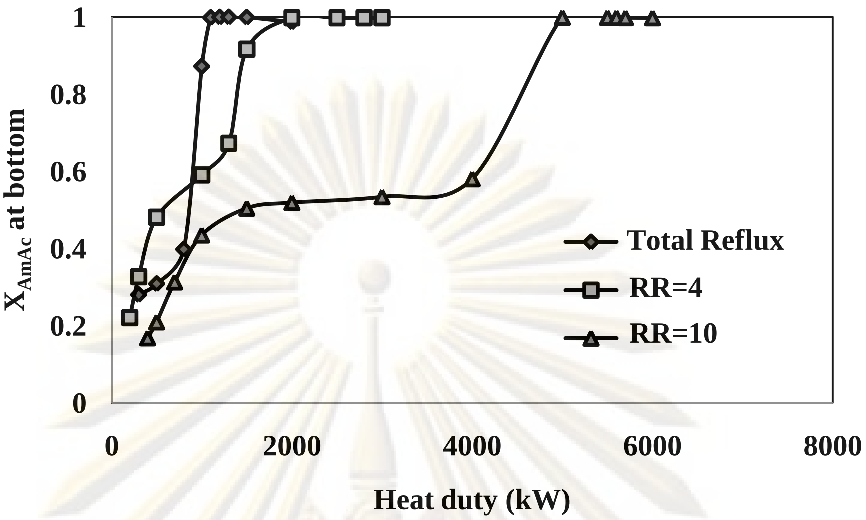

Figure 5.19 Effect of reboiler heat duty on the mole fraction of amyl acetate at bottom of the column at various reflux ratio values (single RD with decanter).

5.3.2 Industrial Scale: Economic Study of the Optimal Configuration of Each Catalyst

As pointed out earlier, each catalyst performs different performance due to the difference of their kinetic rate parameters. Hence, the amyl acetate esterification reaction in reactive distillation catalyzed by different catalyst should have different optimal process configurations. The reactive distillation column consists of a rectifier, a stripper, and a reactive section. Obvious design parameters are the number of rectifying tray (N_{Rec}), the number of stripping trays (N_{Strp}), and the number of reactive trays (N_{Rxn}). In addition to the tray numbers, the important design parameter to compare the performance of the catalysts with the economic consideration is the reactive tray number.

In the simulation, it is noted that the design and operating variables such as number of rectifying tray, number of stripping tray, reactant feed trays and reflux ratio were kept constant as standard condition while reboiler duty, diameter of the column and number of reaction tray were varied to achieve the highest acetic acid conversion, yield and mole fraction of amyl acetate at bottom. Mole fraction of the obtained amyl acetate at bottom was expected at not less than 0.98 along with the commercial grade. The amyl alcohol which is a heavier reactant was introduced in the top of reaction, tray 2 section and acetic acid was fed in the tray 5 which both trays are in the reaction section. As diluted acetic acid aqueous solutions are produced as by-products of many important processes, 35 wt% aqueous solution of acetic acid as a feed stream was used in this simulation system.

The total annual cost (TAC) of Douglas, 1988, Fahmy, 2002 and Hung, 2006 is used to evaluate different RD designs of each catalyst. The TAC is defined as operating cost and capital cost where the operating cost includes the costs of steam, cooling water, and catalyst, and the capital cost covers the cost of the column, trays, and heat exchangers. Appendix D gives the detailed step for computing the TAC. In this work, a payback year of 3 is used and the catalyst life of 3 months is also assumed.

An optimum column reactive distillation fed amyl alcohol and 35 wt% acetic acid was determined. The TAC calculations were carried out for columns with 1 rectifying stage (N_{Rec}), 6 stripping stages (N_{Strp}) and different numbers of reaction (N_{Rxn}) stages for each catalyst; Amberlyst15, Dowex and Beta Zeolite. For each case, the reboiler heat duty was varied until satisfying the bottom product specification of 98 mol% of amyl acetate. Figure 5.20 shows the total annual cost (TAC) at different N_{Rxn} for the case with N_{Rec} = 1 and N_{Strp} = 6. It is obvious that TAC decreases with the increasing number of reaction stage and then slightly increases at higher values. From this case the minimum TAC for Amberlyst15 is observed at N_{Rec} = 1, N_{Rxn} = 15 and N_{Strp} = 6. A similar trend is also observed for Dowex and Beta Zeolite. Figure 5.21 and 5.22 show composition profile for aqueous acetic acid recovery via a single reactive distillation column and temperature profile in liquid phase along the reactive distillation column using Amberlyst 15. Figures 5.24-5.26 show the similar results for Dowex at N_{Rec} = 1, N_{Rxn} = 27 and N_{Strp} = 6 and for Figure 5.27-5.29 for Beta Zeolite N_{Rec} = 1, N_{Rxn} = 31 and N_{Strp} = 6. It is hence observed that the optimum configuration of reactive distillation for the case with 35% acetic acid feed is at N_{Rec} = 1, N_{Rxn} = 15 and N_{Strp} = 6 and catalyzed by Amberlyst 15 with the value of TAC of 343,423 \$/year. Details of the optimum reactive distillation columns of each catalyst are summarized in Table 5.3.

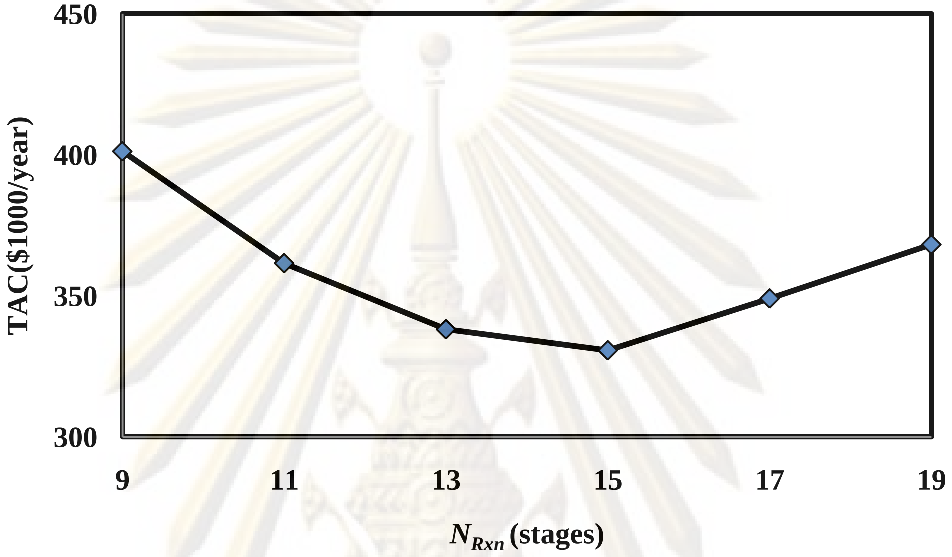

Figure 5.20 Effect of number of reactive tray on the TAC using Amberlyst 15.

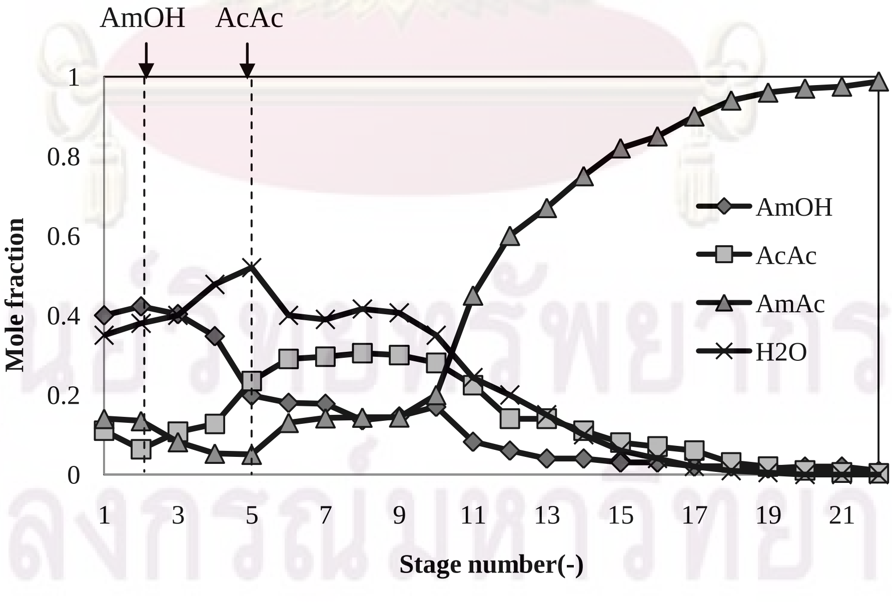

Figure 5.21 Composition profile for aqueous acetic acid recovery via a single reactive distillation column using Amberlyst 15.

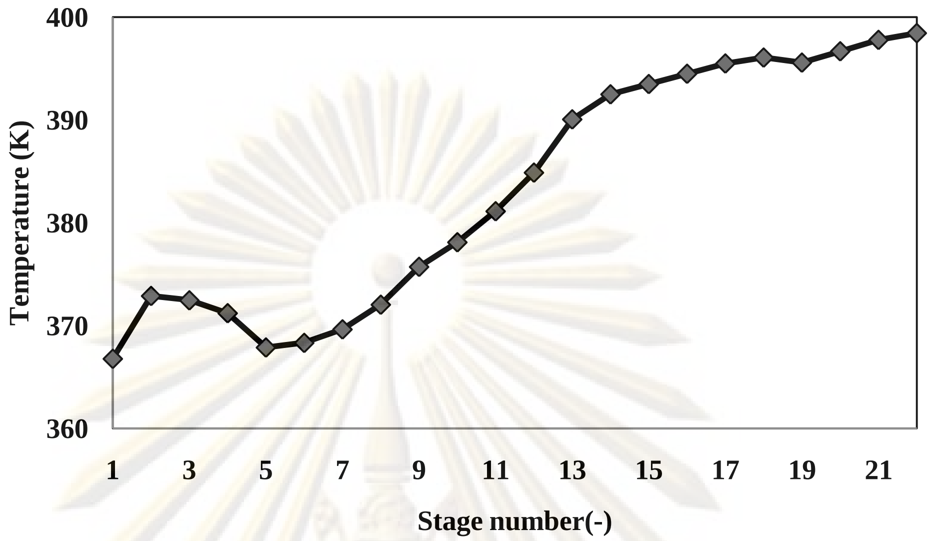

Figure 5.22 Temperature profile in liquid phase along the reactive distillation column using Amberlyst 15.

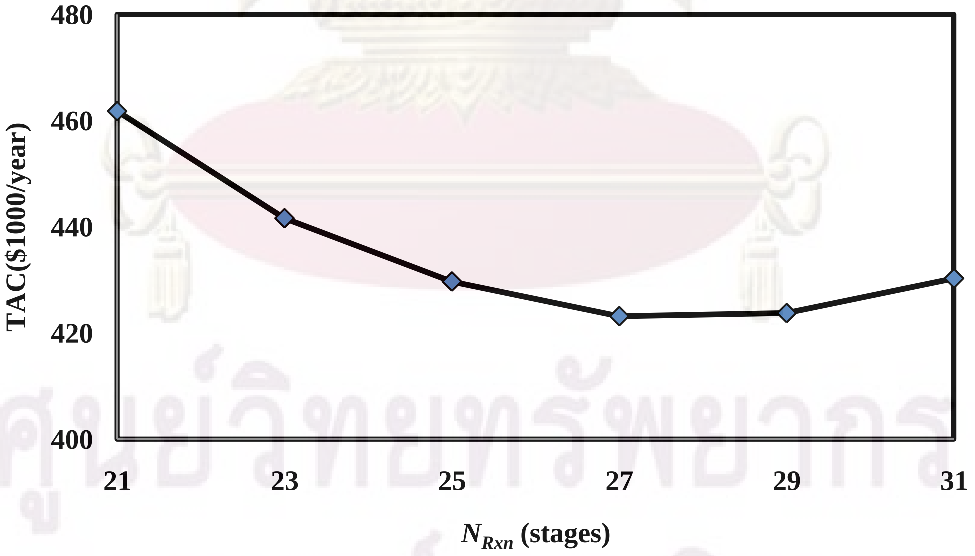

Figure 5.23 Effect of number of reactive tray on the TAC using Dowex.

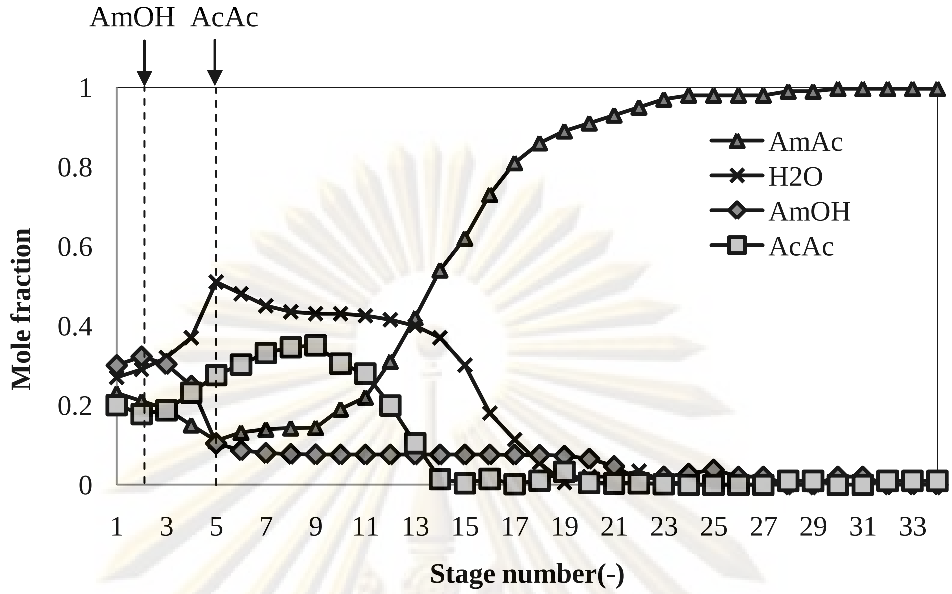

Figure 5.24 Composition profile for aqueous acetic acid recovery via a single reactive distillation column using Dowex.

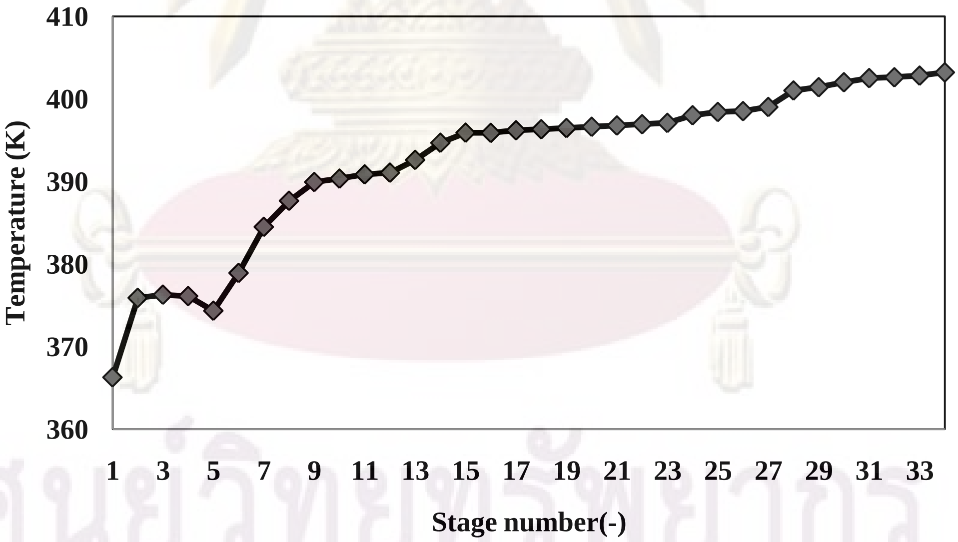

Figure 5.25 Temperature profile in liquid phase along the reactive distillation column using Dowex.

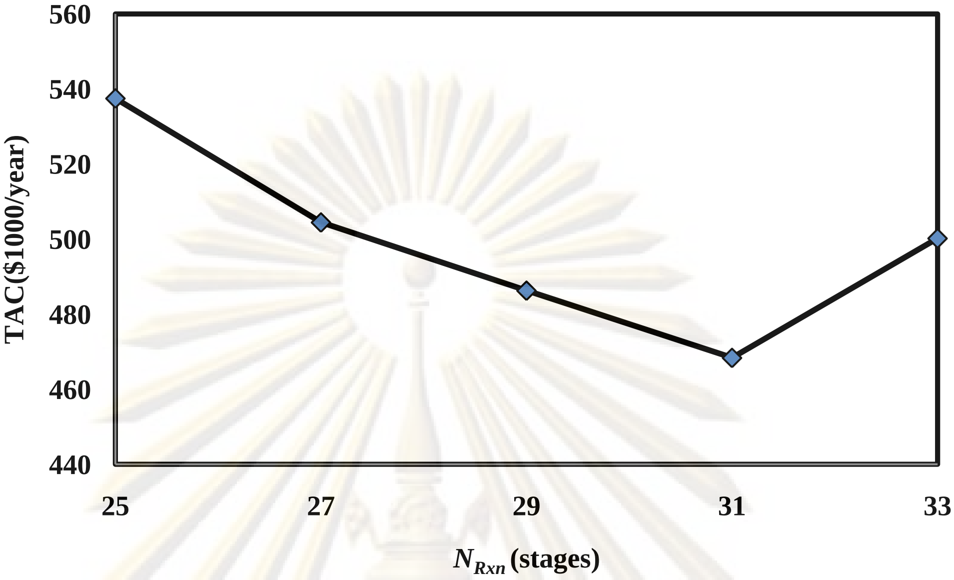

Figure 5.26 Effect of number of reactive tray on the TAC using Beta Zeolite.

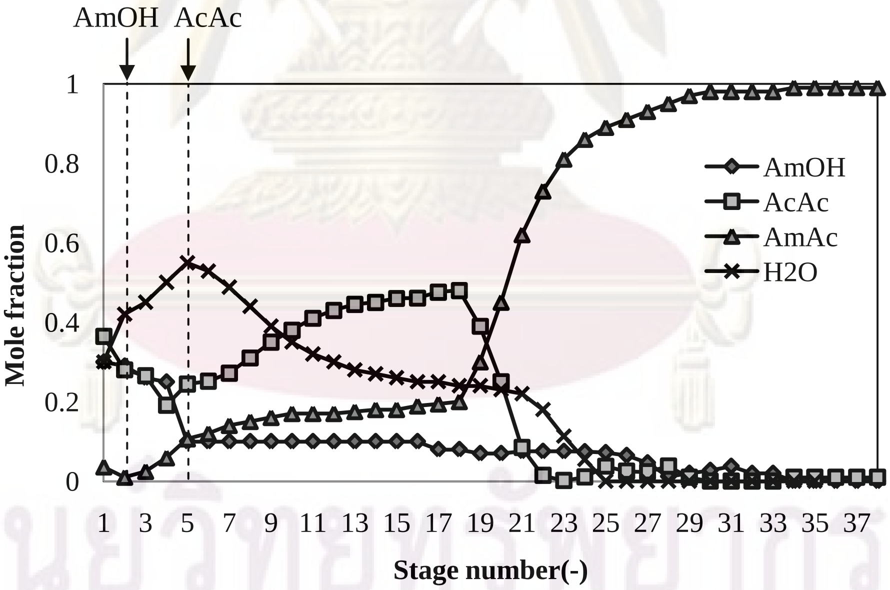

Figure 5.27 Composition profile for aqueous acetic acid recovery via a single reactive distillation column using Beta Zeolite.

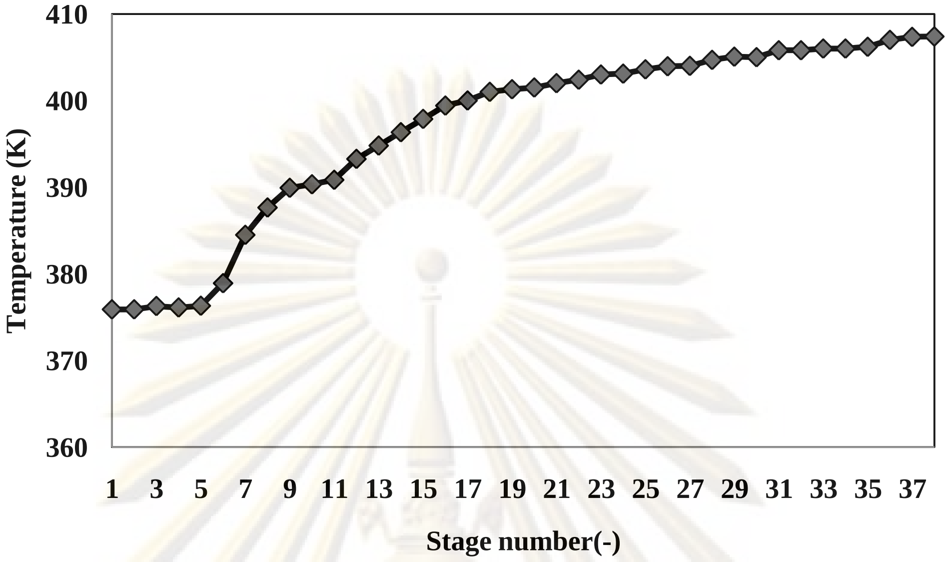

Figure 5.28 Temperature profile in liquid phase along the reactive distillation column using Beta Zeolite.

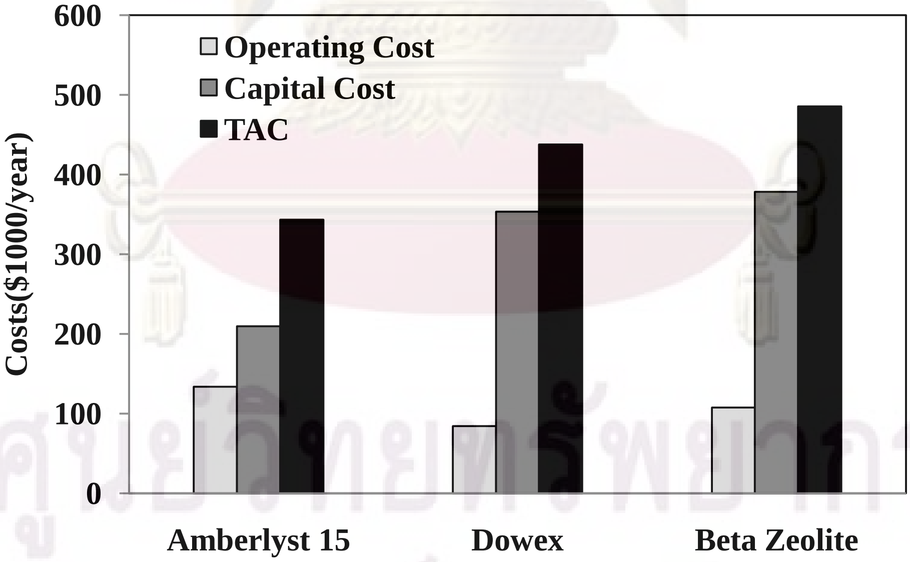

Figure 5.29 Effect of catalysts on capital and operating cost for single reactive distillation with decanter (50 kmol/h acetic acid feed)

Table 5.3 Parameters and results from simulation for amyl acetate synthesis by using difference catalyst in single reactive distillation column.

Parameters	Amberlyst 15	Dowex	Beta Zeolite
Feed flowrate (kmol/hr)			
AcAc	50	50	50
AmOH	50	50	50
N_{Rec}, N_{Rxn}, N_{Strp} (stages)	1, 15, 6	1, 27, 6	1, 31, 6
Mole fraction in RD			
Distillate			
$x_{\mathrm{dist,\ AcAc}}$	0.002	0.003	0.008
$x_{\mathrm{dist,\ AmOH}}$	0.004	0.004	0.002
$x_{\mathrm{dist,\ AmAc}}$	0.008	0.002	0.002
$x_{\mathrm{dist,\ H2O}}$	0.986	0.991	0.988
Bottom			
$x_{\mathrm{bot,\ AcAc}}$	0.010	0.000	0.010
$x_{\mathrm{bot,\ AmOH}}$	0.010	0.010	0.010
$x_{\mathrm{bot,\ AmAc}}$	0.980	0.990	0.980
$x_{\mathrm{bot,\ H2O}}$	0.000	0.000	0.000
Conversion of AcAc (%)	96.234	97.343	94.928
Yield of AmAc (%) at bottom	95.431	93.458	94.254
Condenser duty (kW)	5,490.251	1,368.001	1,610.345
Reboiler duty (kW)	2,965.724	1,696.159	2,203.566
Column diameter (m)	2.25	3.30	3.34
Condenserheat-transfer area (m^2)	97.984	121.904	299.461
Reboiler heat-transfer area (m^2)	127.846	137.485	327.732
Catalyst weight (kg)	577.268	625.425	1,368.438
Capital cost ($1000/year)			
Column	413.363	840.905	891.702
Column trays	48.987	129.269	139.367
Heat exchanger	166.330	89.664	103.617
Operating cost ($1000/year)			
Steam	111.472	63.753	82.825
Cooling	5.365	1.337	1.574
Catalyst	17.026	19.211	23.056
TAC ($1000/year) (50 kmol/h AcAc feed)	**343.423**	**437.580**	**485.683**

CHAPTER VI

CONCLUSION AND RECOMMENDATION

6.1 Conclusions

The application of reactive distillation for production of amyl acetate from amyl alcohol and acetic acid was studied in this thesis. The liquid phase reaction taking place in the reactor systems can be summarized as follows;

$$\mathrm{AmOH + AcAc} \underset{k_b}{\overset{k_f}{\rightleftharpoons}} \mathrm{AmAc + H_2O} \tag{6.1}$$

This work is divided into two parts; experimental studies to find the kinetic rate of the amyl acetate esterification catalyzed by Beta Zeolite and simulation studies which is separated into two section; first, batch reactor, to compare between the results of the reaction in of three catalysts; Beta Zeolite, Amberlyst 15 and Dowex at each temperature and second, reactive distillation in which various process configurations and operating variables of the reactive distillation systems were investigated in order to find their effects on reaction performances as well as their energy consumption and economic analysis. The computer simulations were carried out using Aspen Plus program.

6.2 Kinetic Study

Form kinetics study of amyl acetate esterification from amyl alcohol and acetic acid in the autoclave type reactor at 4 atm. Three temperature levels of 333, 343, and 353 K were used in the study to obtain the parameters in the Arrhenius’s equation for the reaction rate constant and the Van’t Hoff equation for water sorption equilibrium. The reactor was operated at the maximum agitation speed at 1163 rpm to avoid the external mass transfer. The experimental results were fitted with two kinetics models on both activity and concentration base model of Langmuir-Hinshelwood (LH) and Power Law (PL). The repeated reaction schemes of PL and LH models were compared through the values of RMSD. The experimental results agree well with the simulation results for both PL and LH kinetic model. However, the LH-A model which takes into account the effect of water adsorption is the best kinetic model to fit the experimental results.

6.3 Catalyst Performance Comparison

The catalyst performance at various temperature, 360, 380 and 400 K can be compared by acetic acid conversion change with time. It appears that the catalysts have the same tendency that the equilibrium conversion increases with increasing temperature due to the endothermic reaction. The equilibrium conversions of all three catalysts are almost the same while Beta Zeolite catalyst can make the conversion of acetic acid reach the equilibrium before Dowex and Amberlyst 15 catalyst, respectively.

6.4 Reactive Distillation Study

The liquid phase synthesis of amyl acetate from amyl alcohol and acetic acid in reactive distillation column has been studied in this thesis. The simulation of this process using a rate-based kinetic expression and an equilibrium stage model are performed by Aspen Plus program. The influences of design variables on the performance of the reactive distillation are investigated. Various operating parameters; i.e. reflux ratio, heat duty, number of reactive tray and type of catalyst usage were investigated. For the effect of operating parameter, feed flow rate and reflux ratio have significant effect on the performance of reactive distillation. From this study, when the feed flow rate and reflux ratio are increased, the selectivity and conversion was decrease. The suitable reactive distillation configuration for Amberlyst 15 consists of 1 rectifying stage, 15 reaction stages and 6 stripping stage, for Dowex, the column consists of 1 rectifying stage, 27 reaction stages and 6 stripping stage and for the Beta Zeolite catalyst, the column consists of 1 rectifying stage, 31 reaction stages and 6 stripping stage. The total annual cost for each efficient configuration for each catalyst was calculated. A payback year of 3 is used and the catalyst life of 3 months is also assumed. It was clearly demonstrated that the use of different type of catalyst in the reactive distillation made a significant difference in term of TAC. It is found that Amberlyst 15 performed the best performance at the lowest cost follow with Dowex and Beta Zeolite.

6.5 Recommendation

From the simulations of amyl acetate production in this work, it was recommended that some operating parameters such as operating pressure, feed stage location, feed flow rate, more type of catalyst and pre-treatment unit should be further taken into account in the studies as these parameters should influence the reactive distillation performance and total annual cost. In addition, because the dilute acetic acid may be present in different concentration ranges other than 35 wt%, more detailed analysis should be carried out.

REFERENCES

Bianchi, C. L.; Ragaini, V.; Pirola, C.; and Carvoli, G. A new method to clean industrial water from acetic acid via esterification. Appl. Catal. 40 (2003): 93-99.

Chang, Y. C. Feasibility Study on Preparation of Amyl Acetate via Reactive Distillation. Master's Thesis, National Tsing Hua University, Hsinchu, Taiwan, 1997.

Chiang, S. F.; Kuo, C. L.; Yu, C. C.; and Wong, D. S. H. Design Alternatives for Amyl Acetate Process: Coupled Reactor/Column and Reactive Distillation. Ind. Eng. Chem. Res. 41 (2002): 3233-3246.

Chien, I. L.; Zeng, K. L.; Chao, H. Y.; and Liu, J. H. Design and Control of Acetic Acid Dehydration System via Heterogeneous Azeotropic Distillation. Chemical Engineering Science 59 (2004): 4547-4567.

Demiral, H.; and Yildirim, M. E. Recovery of acetic acid from waste streams by extractive distillation. Water Sci. Technol. 47 (2003): 183-188.

Esquivel, M. M.; and Bernardo-Gil, M. G. Liquid-Liquid Equilibria for the Systems: Water/1-Pentanol/Acetic Acid and Water/ 1-Hexanol/Acetic Acid. Fluid Phase Equilib. 62 (1991): 97.

Hung W.J.; Lai I.K.; Hung S.B.; Huang H.P.; Lee M.J.; and Yu, C.C. Control of reactive distillation columns for amyl acetate production using dilute acetic acid. Journal of Molecular Catalysis A: Chemical 226 (2005): 129–134.

Hung, W.J.; Lai I.K.; Hung S.B.; Huang H.P; Lee M.J; and Yu, C.C. Control of reactive distillation columns for amyl acetate production using dilute acetic acid. Journal of the Chinese Institute of Engineers 29 (2006): 319-335.

Lee, J. W.; Hauan, S.; and Westerberg, A. W. Graphical Methods for Reaction Distribution in a Reactive Distillation Column. AIChE J. 46 (2000): 1218.

Lee, L. S.; and Liang, S. C. Phase and Reaction Equilibria of Acetic Acid-1-Pentanol-Water-n-Amyl Acetate System at 760 mmHg. Fluid Phase Equilib. 149 (1998): 57.

Lee, M. J.; Wu, H. T.; Kang, C. H.; and Lin, H. M. Kinetic Behavior of Amyl Acetate Synthesis Catalyzed by Acidic Cation Exchange Resin. J. Chin. Inst. Chem. Eng. 30 (1999): 2.

Lee, M. J.; Chen, S. L.; Kang, C. H.; and Lin, H. M. Simultaneous Chemical and Phase Equilibria for Mixture of Acetic Acid, Amyl Alcohol, Amyl Acetate, and Water. Ind. Eng. Chem. Res. 39 (2000): 11.

Lee, M. J.; Wu, H. T.; and Lin, H. M. “inetics of Catalytic Esterification of Acetic Acid and Amyl Alcohol over Dowex. Ind. Eng. Chem. Res. 39 (2000): 4094.

Palani, Pandurangan. Esterification of acetic acid over mesoporous Al-MCM-41 molecular sieves. Journal of Molecular Catalysis A: Chemical. 226 (2005): 129–134.

Saha, B.; Chopade, S. P.; and Mahajani, S. M. Recovery of Dilute Acetic Acid through Esterification in a Reactive Distillation Column. Catal. Today. 60 (2000): 147-157.

Tang, Y. T.; Hung, S. B.; Chen, Y. W.; Huang, H. P.; Lee, M. J.; and Yu, C. C. Design of Reactive Distillations for Acetic Acid Esterification with Different Alcohols. AIChE J. 51(2005): 1683-1699.

Xu, Z. P.; Afacan, A.; and Chuang, K. T. Removal of Acetic Acid from Water by Catalytic Distillation. Part 1: Experimental Studies. Can. J. Chem. Eng. 77 (1999): 676-681.

Xu, Z. P.; Afacan, A.; and Chuang, K. T. Removal of Acetic Acid from Water by Catalytic Distillation. Part 2: Modeling and Simulation Studies. Can. J. Chem. Eng. 77 (1999): 682-687.

APPENDICES

APPENDIX A

UNIFAC METHOD

The basic idea of the UNIFAC (Universal Quasi-Chemical Functional-Group Activity Coefficient) method is that the behavior of a solution is expressible not by the interactions between molecules but by interaction between their functional groups. In other words, the solution is considered to be a mixture of functional group, not of molecules. Nevertheless, it should be understood that all group contribution methods are necessarily approximate because any group within a molecule is not completely independent of the other groups within that molecule. The UNIFAC for estimation of activity coefficient depends on the concept that a liquid mixture may be considered as a solution of the structural units from which the molecules are formed rather than a solution of the molecules themselves. These structural units are called subgroups, and some of them are listed in the second column of Table A.1. A number, designated k, identifies each subgroup. The relative volume R_k and relative surface area Q_k are properties of the subgroups, and values are listed in column 4 and 5 of Table A.1. When it is possible to construct a molecule from more than one set of subgroups, the set containing the least member of different subgroups is the correct set.

The advantages of the UNIFAC method are as follows;

1. Theory is based on UNIQUAC method.
2. Parameters are essentially independent of temperature.
3. Size and binary interaction parameters are available for wide range of types of functional groups.
4. Prediction can be made over a temperature range of 275 to 425 K and for pressure up to a few atmospheres.
5. Extensive comparisons with experimental data are available.

Activity coefficients depend not only on the subgroup properties R_k and Q_k, but also on interactions between subgroups. Here, similar subgroups are assigned to a main group, as shown in the first two columns of Table A.1. The designations of main groups, such as "CH_2", "ACH", etc., are descriptive only. All subgroups belonging to the same main group are considered identical with respect to group interactions. Therefore parameters characterizing group interactions are identified with pairs of main groups. Parameter value a_{mk} for a few such pairs are given in Table A.2.

The UNIFAC method is based on the UNIQUAC equation which treats $g \equiv G^E / RT$ as comprising of two additive parts, a *combinatorial* term g^C to account for molecular size and shape differences, and a *residual* term g^R to account for molecular interactions:

$$g = g^C + g^R \qquad \text{(A.1)}$$

Function g^C contains pure-species parameters only, whereas function g^R incorporates two binary parameters for each pair of molecules. For a multi-component system,

$$g^C = \sum x_i \ln \frac{\phi_i}{x_i} + 5 \sum q_i x_i \ln \frac{\theta_i}{\phi_i} \qquad \text{(A.2)}$$

and

$$g^R = -\sum q_i x_i \ln(\sum \theta_j \tau_{ji}) \qquad \text{(A.3)}$$

where

$$\phi_i = \frac{x_i r_i}{x_j r_{j\ i}} \qquad \text{(A.4)}$$

and

$$\theta_i = \frac{x_i q_i}{x_j q_{j\ i}} \qquad \text{(A.5)}$$

Subscript *i* identifies species, and *j* is a dummy index; all summations are over all species. Note that $\tau_{ji} \neq \tau_{ii}$; however, when $i = j$, then $\tau_{jj} = \tau_{ii} = 1$. In these equations r_i (a relative molecular volume) and q_i (a relative molecular surface area) are pure-species parameters. The influence of temperature on *g* enters through the interaction parameters τ_{ji} of Equation A-3, which are temperature dependent:

$$\tau_{ji} = \exp \frac{-(u_{ji} - u_{ii})}{RT} \qquad \text{(A.6)}$$

Parameters for the UNIQUAC equation are therefore values of $(u_{ji} - u_{ii})$.

An expression for $\ln \gamma_i$ is applied to the UNIQUAC equation for *g* [Equation A-1 to A-3]. The result is given by the following equations:

$$\ln \gamma_i = \ln \gamma_i^C + \ln \gamma_i^R \qquad \text{(A.7)}$$

$$\ln \gamma_i^C = 1 - J_i + \ln J_i - 5q_i (1 - \frac{J_i}{L_i} + \ln \frac{J_i}{L_i}) \qquad \text{(A.8)}$$

and

$$\ln \gamma_i^R = q_i (1 - \ln s_i - \sum \theta_j \frac{\tau_{ij}}{s_j}) \qquad \text{(A.9)}$$

where in addition to Equation A-5 and A-6

$$J_i = \frac{r_i}{\sum x_j r_j} S \qquad \text{(A.10)}$$

$$L_i = \frac{q_i}{\sum x_j q_j} S \qquad \text{(A.11)}$$

$$s_i = \sum \theta_l \tau_{li} \qquad \text{(A.12)}$$

Again subscript *i* identifies species, and *j* and *l* are dummy indices. All summations are over all species, and $\tau_{ij}=1$ for $i=j$. Values for the parameters $(u_{ij} - u_{jj})$ are found by regression of binary VLE data.

When applied to a solution of groups, the activity coefficients are calculated by:

$$\ln\gamma_i = \ln\gamma_i^C + \ln\gamma_i^R \tag{A.13}$$

when

$$\ln\gamma_i^C = 1 - J_i + \ln J_i - 5q_i(1 - \frac{J_i}{L_i} + \ln\frac{J_i}{L_i}) \tag{A.14}$$

and

$$\ln\gamma_i^R = q_i[1 - (\theta_k\frac{\beta_{ik}}{s_k} - e_{ki}\ln\frac{\beta_{ik}}{s_k})] \tag{A.15}$$

The quantities J_i and L_i are given by:

$$J_i = \frac{r_i}{x_j r_j} \tag{A.16}$$

$$L_i = \frac{q_i}{x_j q_j} \tag{A.17}$$

In addition, the following definition of parameters in Equations A.14 and A.15 apply:

$$r_i = v_k^{(i)} R_k \tag{A.18}$$

$$q_i = v_k^{(i)} Q_k \tag{A.19}$$

$$e_{ki} = \frac{v_k^{(i)} Q_k}{q_i} \tag{A.20}$$

$$\beta_{ik} = e_{mi} \tau_{mk} \tag{A.21}$$

$$\theta_{ik} = \frac{x_i q_i e_{ki}}{x_j q_j} \tag{A.22}$$

$$s_k = \theta_m \tau_{mk} \tag{A.23}$$

$$\tau_{mk} = \exp(\frac{-a_{mk}}{T}) \tag{A.24}$$

Subscript i identified species, and j is a dummy index running over all species. Subscript k identifies subgroups, and m is a dummy index running over all subgroups. The quantity $v_k^{(i)}$ is the number of subgroups of type k in a molecule of species i. Values of the subgroup parameters R_k and Q_k and of the group interaction parameters, a_{mk} come from tabulation in the literature. Tables A.1 and A.2 show parameter values.

Table A.1 UNIFAC-VLE subgroup parameters[†]

Main group	**Subgroup**	**Group name**	**Rk**	**Qk**
1	1	CH_3	0.9011	0.848
1	2	CH_2	0.6744	0.540
1	3	CH	0.4469	0.228
1	4	C	0.2195	0.000
2	5	CH_2=CH	1.3454	1.176
2	6	CH=CH	1.1167	0.867
2	7	CH_2=C	1.1173	0.988
2	8	CH=C	0.8886	0.676
2	9	C=C	0.6605	0.485
3	10	ACH	0.5313	0.400
3	11	AC	0.3652	0.120
4	12	$ACCH_3$	1.2663	0.968
4	13	$ACCH_2$	1.0396	0.660
4	14	ACCH	0.8121	0.348
5	15	OH	1.0000	1.200
6	16	CH_3OH	1.4311	1.432
7	17	H2O	0.9200	1.400
8	18	ACOH	0.8952	0.680
9	19	CH_3CO	1.6724	1.488
9	20	CH_2CO	1.4457	1.180
10	21	CHO	0.9980	0.948
11	22	CH_3COO	1.9031	1.728
11	23	CH_2COO	1.6764	1.420
12	24	HCOO	1.2420	1.188
13	25	CH_3O	1.1450	1.088
13	26	CH_2O	0.9183	0.780
13	27	CH-O	0.6908	0.468
13	28	FCH_2O	0.9183	1.100
14	29	CH_3NH_2	1.5959	1.544
14	30	CH_2NH_2	1.3692	1.236
14	31	$CHNH_2$	1.1417	0.924
15	32	CH_3NH	1.4337	1.244
15	33	CH_2NH	1.2070	0.936
15	34	CHNH	0.9795	0.624
16	35	CH_3N	1.1865	0.940
16	36	CH_2N	0.9597	0.632
17	37	$ACNH_2$	1.0600	0.816
18	38	C_5H_5N	2.9993	2.113
18	39	C_5H_4N	2.8332	1.833
18	40	C_5H_3N	2.6670	1.553
19	41	CH_3CN	1.8701	1.724
19	42	CH_2CN	1.6434	1.416
20	43	COOH	1.3013	1.224
20	44	HCOOH	1.5280	1.532
21	45	CH_2Cl	1.4654	1.264
21	46	CHCl	1.2380	0.952
21	47	CCl	1.0060	0.724

Table A.2 UNIFAC-VLE Group Interaction Parameters, a_{mk}, in kelvins[†]

a_{mk}	**k**	**1**	**2**	**3**	**4**	**5**	**6**	**7**	**8**	**9**	**10**	**11**	**12**	**13**	**14**	**15**	**16**	**17**	**18**	**19**	**20**
m	**Name**	**CH_2**	**C=C**	**ACH**	**$ACCH_2$**	**OH**	**CH_3OH**	**H_2O**	**ACOH**	**CH_2CO**	**CHO**	**CCOO**	**HCOO**	**CH_2O**	**CNH_2**	**CNH_2**	**$(C)_3N$**	**$ACNH_2$**	**PYRIDINE**	**CCN**	**COOH**
1	**CH_2**	0	86.02	61.13	76.5	986.5	697.2	1318	1333	476.4	677	232.1	741.4	251.5	391.5	225.7	206.6	920.7	287.7	597	663.5
2	**C=C**	-35.36	0	38.81	74.15	524.1	787.6	270.6	526.1	182.6	448.8	37.85	449.1	214.5	240.9	163.9	61.11	749.3	0	336.9	318.9
3	**ACH**	-11.12	3.446	0	167	636.1	637.3	903.8	1329	25.77	347.3	5.994	-92.55	32.14	161.7	122.8	90.49	648.2	-4.449	212.5	537.4
4	**$ACCH_2$**	-69.7	-113.6	-146.8	0	803.2	603.2	5695	884.9	-52.1	586.6	5688	115.2	213.1	0	-49.29	23.5	664.2	52.8	6096	603.8
5	**OH**	156.4	457	89.6	25.82	0	-137.1	353.5	-259.7	84	441.8	101.1	193.1	28.06	83.02	42.7	-323	-52.39	170	6.712	199
6	**CH_3OH**	16.51	-12.52	-50	-44.5	249.1	0	-181	-101.7	23.39	306.4	-10.72	193.4	-128.6	359.3	266	53.9	489.7	580.5	36.23	-289.5
7	**H_2O**	300	496.1	362.3	377.6	-229.1	289.6	0	324.5	-195.4	-257.3	72.87	0	540.5	48.89	168	304	-52.29	459	112.6	-14.09
8	**ACOH**	275.8	217.5	25.34	244.2	-451.6	-265.2	-601.8	0	-356.1	0	-449.4	0	0	0	0	0	119.9	-305.5	0	0
9	**CH_2CO**	26.76	42.92	140.1	365.8	164.5	108.7	472.5	-133.1	0	-37.36	-213.7	-38.47	-103.6	0	0	-169	6201	165.1	481.7	669.4
10	**CHO**	505.7	56.3	23.39	106	-404.8	-340.2	232.7	0	128	0	-110.3	11.31	304.1	0	0	0	0	0	0	0
11	**CCOO**	114.8	132.1	85.84	-170	245.4	249.6	200.8	-36.72	372.2	185.1	0	372.9	-235.7	0	-73.5	0	475.5	0	494.6	660.2
12	**HCOO**	90.49	-62.55	1967	2347	191.2	155.7	0	0	70.42	35.35	-261.1	0	0	0	0	0	0	0	0	-356.3
13	**CH_2O**	83.36	26.51	52.13	65.69	237.7	238.4	-314.7	0	191.1	-7.838	461.3	0	0	0	141.7	0	0	0	-18.51	664.6
14	**CNH_2**	-30.48	1.163	-44.85	0	-164	-481.7	-330.4	0	0	0	0	0	0	0	63.72	-41.11	-200.7	0	0	0
15	**CNH_2**	65.33	-28.7	-22.31	223	-150	-500.4	-448.2	0	0	0	136	0	-49.3	108.8	0	-189.2	0	0	0	0
16	**$(C)_3N$**	-83.98	-25.38	-223.9	109.9	28.6	-406.8	-598.8	0	225.3	0	0	0	0	38.89	865.9	0	0	0	0	0
17	**$ACNH_2$**	1139	2000	247.5	762.8	-17.4	-118.1	-367.8	-253.1	-450.3	0	-294.8	0	0	-15.07	0	0	0	0	-281.6	0
18	**PYRIDINE**	-101.6	0	31.87	49.8	-132.3	-378.2	-332.9	-341.6	-51.54	0	0	0	0	0	0	0	0	0	-169.7	-153.7
19	**CCN**	24.82	-40.62	-22.97	-138.4	-185.4	157.8	242.8	0	-287.5	0	-266.6	0	38.81	0	0	0	777.4	134.3	0	0
20	**COOH**	315.3	1264	62.32	268.2	-151	1020	-66.17	0	-297.8	0	-256.3	312.5	-338.5	0	0	0	0	-313.5	0	0

Subgroup classification for amyl acetate synthesis system

To calculation activity coefficient of each component in amyl acetate esterification from liquid phase of amyl alcohol and acetic acid as shown in Equation 2.1, the subgroups of the relevant species are as follows.

Acetic acid (CH_3COOH) : 1 CH_3, 1 COOH
Amyl alcohol ($C_5H_{11}OH$) : 1 CH_3, 4 CH_2, 1 OH
Amyl acetate ($CH_3COOC_5H_{11}$) : 1 CH_3, 4 CH_2, 1 CH_3COO
Water (H_2O) : 1 H_2O

The parameters used in the UNIFAC calculation for this system are summarized in Table A.3 and Table A.4.

Table A.3 UNIFAC-VLE subgroup parameters (for amyl acetate esterification system)†

Group	Main Group	Subgroup (k)	Rk	Qk
CH_3	1	1	0.9011	0.848
CH_2	1	2	0.6744	0.540
OH	5	15	1.0000	1.200
H_2O	7	17	0.9200	1.400
CH_3COO	11	22	1.9031	1.728
COOH	20	43	1.3013	1.224

Table A.4 UNIFAC-VLE interaction parameters, a_{mk}, in Kelvins (for amyl acetate esterification system)†

Group	**Main Group**	**a_{mk}**					
		CH_3	**CH_2**	**OH**	**H_2O**	**CH_3COO**	**COOH**
		1	**1**	**5**	**7**	**11**	**20**
CH_3	**1**	0	0	986.5	1318	232.1	663.5
CH_2	**1**	0	0	986.5	1318	232.1	663.5
OH	**5**	156.4	156.4	0	353.5	101.1	199
H_2O	**7**	300	300	-229.1	0	72.84	-14.09
CH_3COO	**11**	114.8	114.8	245.4	200.8	0	660.2
COOH	**20**	3153	3153	-151	-66.17	-2563	0

† Adapted from XLUNIFAC Version 1.0

APPENDIX B
CALIBRATION CURVE

The pure component sample was injected into the gas chromatography (GC) at the different volume; 0, 0.2, 0.4, 0.6, 0.8, 1.0 ml. The analysis was carried out using GC. The operating condition of the GC is shown in Table 4.3. The raw data of chromatograms was modified to get calibration curve and calibration equation.

Table B.1 Molecular weight, density and retention time of each component

Component	Molecular Wight (g/mol)	Density (g/ml)	Retention Time (min)
AcAc	60.05	1.05	6.69
AmOH	88.15	0.82	21.95
AmAc	130.19	0.87	57.67
H2O	18.00	1.00	1.44

$$Density(g/ml) = \frac{Weight(g)}{Volumn\ (ml)} \tag{B.1}$$

$$Density(g/ml) = \frac{Molecular\ \ Weight\left(\frac{g}{mol}\right)\ x\ Mole\ (mol)}{Volumn\ \ (ml)} \tag{B.2}$$

$$Mole(mol) = \frac{Density\ \left(\frac{g}{ml}\right)\ x\ Volumn\ \ (ml)}{Molecular\ \ Weight(g/mol)} \tag{B.3}$$

Table B.2 Peak area of each component at different volume from Gas Chromatography analysis

Component	Volume (ml)	Area			
		1	2	3	Mean
AcAc	0.00	0.00	0.00	0.00	0.00
	0.20	155674.00	169458.00	195486.00	173539.33
	0.40	341068.00	369748.00	344215.00	351677.00
	0.60	524951.00	564444.00	552170.00	547188.33
	0.80	728704.00	732290.00	739568.00	733520.67
	1.00	918622.00	932240.00	895129.00	915330.33
AmOH	0.00	0.00	0.00	0.00	0.00
	0.20	106715.00	100105.00	111361.00	106060.33
	0.40	236501.00	237013.00	229251.00	234255.00
	0.60	373065.00	376337.00	385290.00	378230.67
	0.80	496711.00	523703.00	487061.00	502491.67
	1.00	625477.00	686673.00	640454.00	650868.00
AmAc	0.00	0.00	0.00	0.00	0.00
	0.20	101571.00	134071.00	102512.00	112718.00
	0.50	291104.00	202970.00	252665.00	248913.00
	0.60	359731.00	395631.00	366356.00	373906.00
	0.80	488154.00	507642.00	499695.00	498497.00
	1.00	666912.00	668985.00	616707.00	650868.00
H_2O	0.00	0.00	0.00	0.00	0.00
	0.20	229387.00	224955.00	240682.00	231674.67
	0.40	523675.00	501784.00	505034.00	510164.33
	0.60	799968.00	797563.00	798736.00	798755.67
	0.80	1065871.00	1079518.00	1080647.00	1075345.33
	1.00	1354630.00	1344140.00	1357753.00	1352174.33

From Equation B.3, mole of each component can be calculated from density, volume and molecular weight.

Acetic acid at 0.2 ml;

$$Mole(mol) = \frac{1.05(\frac{g}{ml})\ x\ 0.2(ml)}{60.05(g/mol)}$$

$$= 0.3497\ x\ 10^{-2}$$

Table B.3 Data of Peak area and mole of acetic acid for the calibration curve

Volume(ml)	Peak Area	Mole(x10^{-2})
0.0	0	0
0.2	173539	0.3497
0.4	351677	0.6994
0.6	547188	1.0491
0.8	733521	1.3988
1.0	915330	1.7485

From Table B.3, the calibration curve can be plotted as shown in Figure B.1

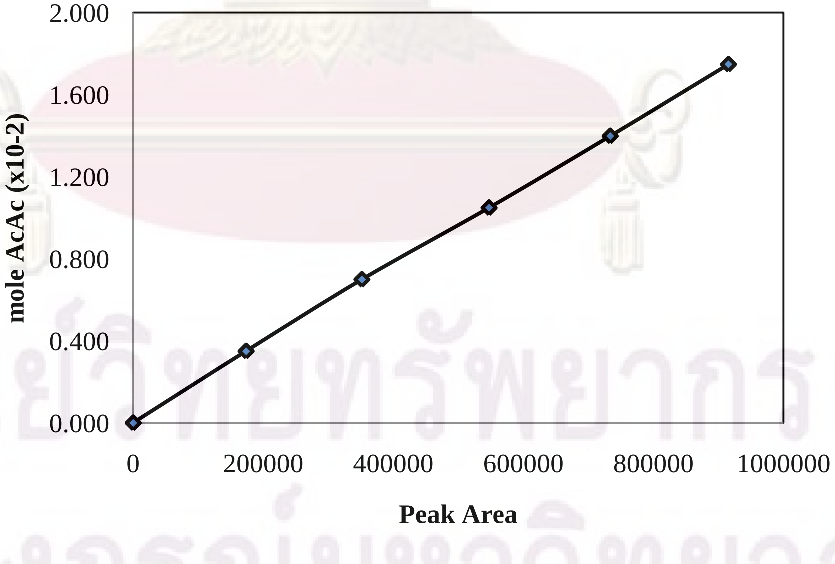

Figure B.1 Calibration curve between peak area and mole of acetic acid

From Figure B.1, the equation of calibration curve can be summarized as shown in Table B.4;

Table B.4 Calibration equation of each component

Component	**Calibration equation**
AmOH	Mole = (1.416 x 10^{-4})Peak Area + 2.323
AmAc	Mole = (1.896 x 10^{-4})Peak Area + 1.414
AcAc	Mole = (1.030 x 10^{-4})Peak Area + 1.068
H_2O	Mole = (4.056 x 10^{-4})Peak Area + 9.558

APPENDIX C

KINETIC EQUILIBRIUM CONSTANT CALCULATION FROM GIBBS ENERGY OF FORMATION

The amyl acetate synthesis reaction takes place in the direct esterification of amyl alcohol and acetic acid which can be seen as below.

$$\text{AmOH} + \text{AcAc} \underset{k_b}{\overset{k_f}{\longleftrightarrow}} \text{AmAc} + H_2O \tag{C.1}$$

For the kinetic equilibrium constant, it is defined as;

$$K_{eq} = \frac{k_f}{k_b} \tag{C.2}$$

Where f = forward reaction and b = backward reaction

Gibbs energy of formation was used to determine the equilibrium parameter, K_{eq}, in term of activity

$$\Delta G_{rxn} = \Delta G_{f,AmAc} + \Delta G_{f,H_2O} - \Delta G_{f,AmOH} - \Delta G_{f,AcAc} \tag{C.3}$$

$$\Delta G_f = A + BT + CT^2 \tag{C.4}$$

Table C.1 Regression coefficient of each compound

Compound	Regression Coefficient		
	A	**B**	**C**
AmOH	-3.052E+02	5.064E-01	4.523E-05
AcAc	-4.360E+02	1.935E-01	1.636E-05
AmAc	-5.094E+02	6.745E-01	4.773E-05
H_2O	-2.417E+02	4.174E-02	7.428E-06

When parameters are substituted in Equation C.3, we can calculate the Gibbs energy of each compound at different temperature as shown in Table C.2 and Gibbs energy of formation of the reaction of amyl acetate synthesis from amyl alcohol and acetic acid can be calculated from Equation C.2, which is summarized in Table C.3.

For AmOH at 303 K;

$$\Delta G_{f,AmAc} = (-305.2) + (0.5064\, x 303) + \ (0.00004523\ x\ 303^2)$$

$$= -147.572\ kJ/mol$$

At 303 K;

$$\Delta G_{rxn} = (-300.596) + (-228.411) - (-147.572) - (-375.842)$$

$$\Delta G_{rxn} = -5.592\ kJ/mol$$

Table C.2 Gibbs energy of each compound at different temperature

Compound	Temperature (K)					
	303	**313**	**323**	**333**	**343**	**353**
AmOH	-147.572	-142.230	-136.878	-131.518	-126.149	-120.770
AcAc	-375.842	-373.807	-371.768	-369.726	-367.681	-365.633
AmAc	-300.596	-293.557	-286.508	-279.450	-272.382	-265.305
H_2O	-228.411	-227.948	-227.483	-227.017	-226.549	-226.080
ΔG_{rxn} (kJ/mol)	-5.592	-5.468	-5.344	-5.222	-5.101	-4.982

Table C.3 Gibbs energy of formation of amyl acetate at various temperatures

Temp(K)	**1000/T**	**ΔG_{rxn}**	**lnK=- ΔG_{rxn} /RT**	**K**
303	3.300	-5.592	2.220	9.206
313	3.195	-5.468	2.101	8.174
323	3.096	-5.344	1.990	7.316
333	3.003	-5.222	1.886	6.594
343	2.915	-5.101	1.789	5.982
353	2.833	-4.982	1.697	5.460

The equilibrium constant in activity form of amyl acetate esterification can be obtained from the Arrhenius' plots between 1000/T and lnK.

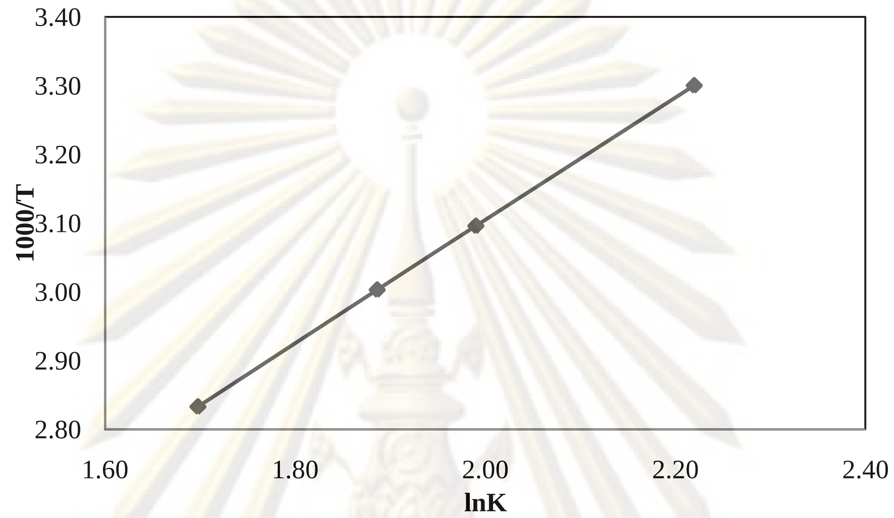

Figure C.1 Arrhenius plots between 1000/T and lnK

Finally, the equilibrium constant in activity form of amyl acetate esterification can be derived as below;

$$K_{eq,a} = exp\left(-1.471 + \frac{1118.568}{T}\right) \tag{C.5}$$

APPENDIX D

SIZING OF EQUIPMENT AND CALCULATION OF COST

Table D.1 Sizing of equipment and catalyst weight calculation

Parameter	Remarks	Equations
A_{Reb} [m^2]	reboiler heat-transfer area	$A_{\mathrm{Reb}} = \dfrac{Q_{\mathrm{Reb}}}{U_{\mathrm{Reb}} \Delta T_{\mathrm{Reb}}}$
A_{Cond} [m^2]	condenser heat-transfer area	$A_{\mathrm{Cond}} = \dfrac{Q_{\mathrm{Cond}}}{U_{\mathrm{Cond}} \Delta T_{\mathrm{Cond}}}$
H [m]	column hight	$H = (\text{tray spacing})(N_{\mathrm{tray}})$
m_{cat} [kg]	catalyst weight	$m_{\mathrm{cat}} = \dfrac{\pi D_{\mathrm{C}}^{2}}{4}(0.9)(h_{\mathrm{weir}})(0.5)(\rho_{\mathrm{cat}})$

Table D.2 Notation and parameter values for sizing of equipment and cost calculation (Hung, 2006).

Parameter	Value	Remarks
C_{MS} [\$]	1,108.1	Marshall and Swift index (as of 2000)
U_{Reb} [W/m^2.K]	788.45	overall heat-transfer coefficient of reboiler
ΔT_{Reb} [K]	25	temperature driving force of reboiler
U_{Cond} [W/m^2.K]	473.07	overall heat-transfer coefficient of condenser
ΔT_{Cond} [K]	calculated	log-mean temperature driving force of condenser (temperature of process stream cooling water inlet and outlet temperature of 32 and 49 $^{\mathrm{o}}$C, respectively)
ρ_{cat} [kg/m^3]	770	catalyst density for Amberlyst 15
h_{weir} [m]	0.1	weir height for tray

Capital and operating costs can be calculated by following the previous work by Douglas, 1988, Fahmy, 2002 and Hung, 2006. Details are as follows:

Capital cost

Column cost

$$\mathrm{Cost,\$} = \left(\frac{C_{\mathrm{MS}}}{280}\right)101.9D^{1.066}H^{0.802}\left(2.18 + F_m F_p\right); \qquad F_m = 3.67,\ F_p = 1.00$$

Tray cost

$$\mathrm{Cost,\$} = \left(\frac{C_{\mathrm{MS}}}{280}\right)4.7D^{1.55}H\left(F_s + F_t + F_m\right); \qquad F_s = 1.00,\ F_t = 0.00,\ F_m = 1.70$$

where D = diameter of the column (ft)

H = high of the column (ft)

Heat-exchanger cost

$$\text{Cost, \$} = \left(\frac{C_{\text{MS}}}{280}\right)101.3A^{0.65}\left(2.29 + \left(F_d + F_p\right)F_m\right); \quad F_d = 1.350 \text{ for reboiler}$$

F_d = 1.000 for condenser, F_p = 0.000, F_m = 3.750

where A = heat transfer area (ft^2)

Operating cost

Steam cost

$$\text{Cost, \$/y} = \left(\frac{\$\,C_s}{1{,}000\,\text{lb}}\right)\left(\frac{Q_{\text{Reb}}}{\Delta H_s}\frac{\text{lb}}{\text{h}}\right)\left(8150\frac{\text{hr}}{\text{y}}\right)$$

where C_s = cost of steam (\$/1,000 lb steam)

Cooling cost

$$\text{Cost, \$/y} = \left(\frac{\$\,C_w}{1{,}000\,\text{gal}}\right)\left(\frac{1}{8.34}\frac{\text{gal}}{\text{lb}}\right)\left(\frac{Q_{\text{Cond}}}{30}\frac{\text{lb}}{\text{h}}\right)\left(8150\frac{\text{hr}}{\text{y}}\right)$$

where C_w = cost of cooling water (\$/1,000 gal cooling water)

Catalyst cost

$$\text{Cost, \$/y} = \left(m_{\text{cat}}\ [\text{kg}]\right)\left(7.7162\frac{\$}{\text{kg}}\right)(4) \text{ for a catalyst life of 3 months}$$

Electricity cost

$$\text{Cost, \$} = \left(\frac{0.04}{\text{kW - h}}\right)$$

Example of calculations

Reactive distillation equipped with decanter system for using acetic acid 35 wt% (50 kmol/h acetic acid feed) and catalyzed by Amberlyst 15

$$A_{\mathrm{Reb}} = \frac{(2{,}965{,}724\,\mathrm{W})}{\left(788.45\,\frac{\mathrm{W}}{\mathrm{m^2K}}\right)(25\,\mathrm{K})} = 150.458\,\mathrm{m}^2 = 1{,}619.52\,\mathrm{ft}^2$$

$$A_{\mathrm{Cond}} = \frac{5{,}490{,}251W}{\left(473.07\,\frac{\mathrm{W}}{\mathrm{m^2K}}\right)(44.849\,\mathrm{K})} = 258.77\,\mathrm{m}^2 = 2{,}785.38\,\mathrm{ft}^2$$

$$H = (\text{tray spacing})(N_{\text{tray}}) = (2\,\mathrm{ft})(22) = 44\,\mathrm{ft}$$

$$\begin{aligned} m_{\mathrm{cat}} &= \frac{\pi\left(2.25^2\ \mathrm{m}^2\right)}{4}(0.9)(0.1\,\mathrm{m})(0.5)\left(770\,\frac{\mathrm{kg}}{\mathrm{m}^3}\right) \\ &= 551.621\,\mathrm{kg} \end{aligned}$$

<u>**Capital cost**</u>

Column cost;

$$\text{Cost} = \left(\frac{1{,}108.1}{280}\right)(101.9)\left(7.383^{1.066}\right)\left(44^{0.802}\right)(2.18 + 3.67) = \$413{,}363.00$$

Tray cost;

$$\text{Cost, \$} = \left(\frac{1{,}108.1}{280}\right)(4.7)\left(7.383^{1.55}\right)(44)(1 + 0 + 1.7) = \$48{,}987.28$$

Heat-exchanger cost;

$$\text{Cost, \$} = \left(\frac{1{,}108.1}{280}\right)(101.3)\left(150.46^{0.65}\right)\left(2.29 + (1.35 + 0)(3.75)\right) = \$76{,}698.93$$

For reboiler

$$\text{Cost, \$} = \left(\frac{1{,}108.1}{280}\right)(101.3)\left(258.77^{0.65}\right)\left(2.29 + (1.000 + 0)(3.75)\right) = \$89{,}631.5$$

For condenser

Operating cost

Steam cost;

$$\text{Cost, \$/y} = \left(\frac{\$\,3.72}{1{,}000\,\text{lb}}\right)\left(\frac{2{,}96{,}724\,\frac{\text{Btu}}{\text{h}}}{806.617\,\frac{\text{Btu}}{\text{lb}}}\right)\left(8150\,\frac{\text{h}}{\text{y}}\right) = \$111{,}472$$

Cooling cost;

$$\text{Cost, \$/y} = \left(\frac{\$\,0.03}{1{,}000\,\text{gal}}\right)\left(\frac{1}{8.34}\,\frac{\text{gal}}{\text{lb}}\right)\left(\frac{5{,}490{,}251}{30}\,\frac{\text{lb}}{\text{hr}}\right)\left(8{,}150\,\frac{\text{hr}}{\text{y}}\right) = \$5{,}365.17$$

Catalyst cost;

$$\text{Cost, \$/y} = \left(551.621[\text{kg}]\right)\left(7.7162\,\frac{\$}{\text{kg}}\right)(4) = \$17{,}025.7$$

So,

$$\begin{aligned} \text{TAC} &= \text{operating cost} + \frac{\text{capital cost}}{\text{pay - back period}} \\ &= 133{,}862.36 + \frac{628{,}680.54}{3} \\ &= \$343{,}422.54 \end{aligned}$$

VITA

Ms. Anchan Paethanom was born on July 25, 1983 in Mae Hong Son, Thailand. She finished high school from Monfort College, Chiang Mai, Thailand. She received Bachelor’s degree of Science in Industrial Chemistry from the department of Chemistry, faculty of Science, Kasetsart University, Bangkok, Thailand in 2005 and Master’s degree of Engineering in Chemical Engineering from the department of Chemical Engineering, faculty of Engineering, Chulalongkorn University, Bangkok, Thailand in 2009.